

Ministry of Higher Education & Scientific Research

Ninevah University

College of Electronics Engineering

Electronic Engineering Department



**Wireless Power Transmission Technology
for Portable Devices**

By

Reem Emad Nafiaa Qreshat

M.Sc.Thesis

In

Electronic Engineering

Supervised by

Asst. Prof. Dr. Aws Zuheer Yonis Alashqar

Ministry of Higher Education & Scientific Research

Ninevah University

College of Electronics Engineering

Electronic Engineering Department



**Wireless Power Transmission Technology
for Portable Devices**

A thesis Submitted

By

Reem Emad Nafiaa Qreshat

To

The Council of the College of Electronic Engineering Ninevah
University

As a Partial Fulfillment of the Requirements for the Degree of Master of
Science

In Electronic Engineering

Supervised by

Asst.Prof.Dr. Aws Zuheer Yonis Alashqar

Committee Certification

We the examining committee, certify that we have read this dissertation entitled **(Wireless Power Transmission Technology for Portable Devices)** and have examined the postgraduate student **(Reem Emad Nafiaa)** in its contents and that in our opinion; it meets the standards of a dissertation for the degree of Master of Science in Electronic Engineering.

Signature:

Name: Assist. Prof. Dr. Ahmad T. Younis
Head of committee

Date:

Signature:

Name: Assist. prof. Dr. Ahmed M. Salama
Member

Date:

Signature:

Name: Dr. Mohamad N. Abdul Kadir
Member

Date:

Signature:

Name: Assist. Prof. Dr. Aws Z. Yonis
Member and Supervisor

Date:

The college council, in its _____ meeting on _____, has decided to award the degree of Master of Science in Electronic Engineering to the candidate.

Signature:

Name: Prof. Khaled Khalil Muhammad
Dean of the Electronic Engineering College

Date:

Signature:

Name: Assist. Prof. Dr. Dia M. Ali
Rapporteur of the Council

Date:

Supervisor's Certification

We certify that the dissertation entitled (**Wireless Power Transmission Technology for Portable Devices**) was prepared by (**Reem Emad Nafiaa**) under our supervision at the Department of Electronic Engineering, Ninevah University, as a partial requirement for the Master of Science Degree in Electronic Engineering.

Signature:

Name: Assist. Prof. Dr. Aws Zuheer Yonis

Date:

Report of Linguistic Reviewer

I certify that the linguistic reviewing of this dissertation was carried out by me and it is accepted linguistically and in expression.

Signature:

Name: Mahfoz khalaf Mahmoud

Date:

Report of the Head of Department

I certify that this dissertation was carried out in the Department of Electronic Engineering. I nominate it to be forwarded to discussion.

Signature:

Name: Prof. Dr. Qais Thanoon Najim

Date:

Report of the Head of Postgraduate Studies Committee

According to the recommendations presented by the supervisors of this dissertation and the linguistic reviewer, I nominate this dissertation to be forwarded to discussion.

Signature:

Name: : Prof. Dr. Qais Thanoon Najim

Date:

ACKNOWLEDGMENTS

I would like to express my sincere gratitude and thanks to my supervisor, Dr. Aws Zuheer Yonis for his helpful guidance and suggestions in addition to the continuous encouragement through this research.

I would like to thank all the teaching staff in the Electronics Engineering Department for their support and assistance, I ask God to bless them.

I would like to extend my sincere appreciation to my father, mother and my husband for their support and encouragement through the duration of my graduate study.

Finally, thanks to everyone who has credited me, even with a letter, advice or assistance.

To all of them I express my sincere appreciation and respect.

ABSTRACT

Wireless power transmission (WPT) technology has now become one of the most important technologies and the focus of scientists. The principle of this technology is to send power from a device called the transmitter to another device called the receiver without using cables. The type of WPT technique that had been used is Inductive coupling, due to its ease of use and safety compared to the traditional transmission techniques .

In this thesis, a wireless system has been designed to be able to transfer power or charge smartphones with 10 Watt, 5V, and 2A using the resonance inductive technique.

The work had been divided as shown below:

Firstly, to clarify the Frequency Splitting Phenomenon, a system had been designed and simulated by ADS program which is considered a problem in WPT, to illustrate the effect of the coupling factor on the system that leads to making this splitting in frequency and reaches that whenever resonance frequency increases the splitting at lower coupling occur.

Secondly, the wireless system for smartphone charging had been designed and simulated by MATLAB program considering some of the factors that have an impact on the system efficiency such as distance, coupling factor, and resonance frequency from 50-100 KHz.

The result indicates that the wireless system that had been designed for charging smartphone applications achieved the better system performance at $f_r=100$ KHz, where the efficiency is equal to 76% when distance between TX and RX is 30 mm whereas at $f_r=50$ KHz with the distance between TX and RX is equal to 30 mm the efficiency reaches to 71%.

LIST OF CONTENTS

Subject		Page
Abstract		I
Table of Contents		II
List of Figures		III
List of Tables		VI
List of Abbreviation		XI
List of Symbols		XII
CHAPTER ONE		
1.1	Introduction	1
1.2	Literature Review	3
1.3	Comparison Between Wireless and Wire Charging	
1.4	Aims of the Thesis	5
1.5	Thesis Outlines	5
CHAPTER TWO		
2.1	Introduction	7
2.2	Applications of wireless power transfer	8
2.3	Wireless Power Transmission Types	9
2.4	Main Concepts of the Resonance Inductive Coupling Wireless Power Transfer System	11
2.4.1	Resonance	12
2.4.2	Quality factor (Q)	14
2.4.3	Coupling Factor	15
2.4.4	Mutual inductance (M)	15
2.5	The Components of Resonance IPT System Achievement	16
2.5.1	Compensation Circuit	17
2.5.2	Inverter	18

Subject		Page
2.5.2.1	Half Bridge Inverter	19
2.5.2.2	Full Bridge Inverter	21
2.5.3	Rectifier	23
2.5.4	Inductive Coils	24
2.6	Smartphone Charging Work Principle	27
2.7	Frequency Splitting Phenomenon	28
CHAPTER THREE		
3.1	Introduction	31
3.2	Design and Simulation of the Proposed System of Frequency Splitting Phenomenon	33
3.2.1	Simulation Results of the Frequency Splitting Phenomenon (FSP).	34
3.2.2	Simulation Results of the Frequency Splitting Phenomenon at $f_r=10$ MHz.	35
3.2.3	Simulation Results of the FSP at $f_r= 20$ MHz.	37
3.2.4	Simulation Results of the Frequency Splitting Phenomenon at $f_r= 30$ MHz.	39
3.2.5	Comparison Results among three Frequencies 10, 20 and 30 MHz.	41
3.3	Coils Parameter Design of WPT Charging System.	41
3.3.1	Circuit Parameter Calculation	44
3.3.2	Resonance Frequency Calculation Code	45
3.4	WPT Proposed Design of Smartphone Charging Application	46

3.5	Simulation Results of the Frequency Variation Effect	53
3.6	Simulation Results of WPT for Smartphone charging System	56
3.6.1	Simulation Results of WPT for Smartphone charging System at Fr =50 KHz	56
3.6.2	Simulation Results of WPT for Smartphone charging System at Fr =60 KHz	58
3.6.3	Simulation Results of WPT for Smartphone charging System at Fr =70 KHz	59
3.6.4	Simulation Results of WPT for Smartphone charging System at Fr =80 KHz	61
3.6.5	Simulation Results of WPT for Smartphone charging System at Fr =100 KHz	62
3.7	Results for Charging Smartphone Battery at Fr=100KHz..	64
3.8	Results Discussion	66
CHAPTER FOUR		
4.1	Conclusions	69
4.2	Future Works	70
REFERENCES		
References		72

LIST OF FIGURES

Figure	Title	Page
1.1	Work principle of WPT system	2
2.1	Typical diagram of WPT for charging battery.	8
2.2	Wireless power transfer applications	9
2.3	Types of Wireless Power Transfer	10
2.4	(a) Inductive coupling, (b) Resonance inductive coupling WPT System.	11
2.5	RLC series circuit	12
2.6	Conventional circuit of resonant inductive coupling system	16
2.7	Schematic diagram of resonance inductive WPT system	17
2.8	Compensation circuit types	18
2.9	Half bridge inverter	19
2.10	Current path at SW1= on , SW2 = off	20
2.11	Current path at SW1= off, SW2 = on	20
2.12	Output voltage VL of half bridge inverter at SW1, SW2	21
2.13	Full bridge inverter	21
2.14	Current path at SW1 and SW4 on	22
2.15	Current path at SW2 and SW3 on	22
2.16	Output voltage VL of half bridge inverter at SW1, SW2	23
2.17	Full bridge rectifier	24
2.18	WPT equivalent circuit	26

2.19	Work principle of wireless charging system	28
2.20	Frequency splitting phenomenon of two coils	29
3.1	Smartphone charging operation technique.	32
3.2	Topology of WPT for FSP design	33
3.3	Efficiency for under coupled range at $K=0.02$, $Fr=10$ MHz	35
3.4	Efficiency for critical coupled range at $K=0.04$, $Fr=10$ MHz	36
3.5	Efficiency for over coupled range at $K=0.05$, $Fr=10$ MHz	36
3.6	Efficiency for critical coupled range at $K=0.02$, $Fr=20$ MHz	38
3.7	Efficiency for over coupled range at $K=0.03$, $Fr=20$ MHz	38
3.8	Efficiency for critical coupled range at $K=0.013$, $Fr=30$ MHz	40
3.9	Efficiency for over coupled range at $K=0.02$, $Fr=30$ MHz	40
3.10	The splitting in frequency among 10, 20 and 30MHz	42
3.11	Coil for wireless charging	43
3.12	Diagram illustrates the notations used for the coils design	43
3.13	Proposed design of smartphone charging applications	48
3.14	Output of inverter I, V at $Fr=100$ KHz	51
3.15	Current and voltage of the secondary coil at $Fr=100$ KHz	51

3.16	The current changing of the input stage at Fr from 70 to 100 KHz	52
3.17	The voltage changing of the input stage at Fr from 70 to 100 KHz	52
3.18	Mutual inductance at distance from 20 to 60mm	54
3.19	Coupling coefficient at distance from 20 to 60mm	55
3.20	MOSFET current at Fr= 50 KHz	56
3.21	Signals of current and voltage at the primary stage of WPT system at Fr= 50 KHz	57
3.22	Signals of current and voltage at the secondary stage of WPT system at Fr= 50 KHz	57
3.23	MOSFET current at Fr=60 KHz	58
3.24	Signals of current and voltage at the primary stage of WPT system at Fr=60 KHz	58
3.25	Signals of current and voltage at the secondary stage of WPT system at Fr= 60 KHz	59
3.26	MOSFET current at Fr= 70 KHz	59
3.27	Signals of current and voltage at the primary stage of WPT system at Fr=70 KHz	60
3.28	Signals of current and voltage at the secondary stage of WPT system at Fr= 70 KHz	60
3.29	MOSFET current at Fr= 80 KHz	61
3.30	Signals of current and voltage at the primary stage of WPT system at Fr= 80 KHz.	62
3.31	Signals of current and voltage at the secondary stage of WPT system at Fr=80 KHz	62
3.32	MOSFET current at Fr=100 KHz	63

3.33	Signals of current and voltage at the primary stage of WPT system at Fr= 100 KHz.	63
3.34	Signals of current and voltage at the primary stage of WPT system at Fr= 100 KHz	64
3.35	Signals of current and voltage at the secondary stage of WPT system at Fr= 60 KHz	64
3.36	Output Dc Current Fr=100 KHz	64
3.37	Output Dc voltage at Fr=100 KHz	65
3.38	Input applied current and voltage at resonance frequency changing	67
3.39	Efficiency at resonance frequency from 50 to 100 KHz	67
3.40	Efficiency at different distances	68

LIST OF TABLES

Table	Title	Page
3.1	Maximum efficiency at three coupling situation at Fr=10 MHz	37
3.2	Maximum efficiency at three coupling situation at Fr= 20 MHz	39
3.3	Maximum efficiency at three coupling situation at Fr= 30 MHz	41
3.4	Parameters of the Smartphone Charging System Coils	44
3.5	Parameters of the WPT circuit of frequency variation simulation	50
3.6	Parameters of the smartphone charger proposed design	54
3.7	Results of the smartphone charging proposed design	66

LIST OF ABBREVIATIONS

Abbreviation	Name
AC	Alternating Current
DC	Direct Current
FSP	Frequency Splitting Phenomenon
IGBT	Insulated Gate Bipolar Transistor
IPT	Inductive Power Transfer
MOSFET	Metal Oxide Semiconductor Field Effect Type
P-P	Parallel- Parallel
P-S	Parallel- Series
PTE	Power Transmitter Efficiency
RICPT	Resonance Inductive Coupling Power Transfer
RX	Receiver
S-P	Series-Parallel
S-S	Series-Series
SW	Switch
TX	Transmitter
WPT	Wireless Power Transfer
XC	Capacitive Reactance
XL	Inductive Reactance

LIST OF SYMBOLS

Symbol	Name
BW	Bandwidth
C	Capacitor
f	Frequency
Fr	Resonance Frequency
ICPT	Inductive coupling power transfer
K	Coupling Factor
L	Inductor
M	Mutual Inductance
Q	Quality Factor
R	Resistance
S1,S2	Cross Section of the Coils
V_{DC}, V_{in}	Input Dc Voltage
V_L	Load Voltage
V_{out}	Output Voltage
V_s	Source Voltage
ω	Angular Frequency
ω_o	Angular Resonance Frequency
Z	Impedance

μ_0	Permeability of the Air
D	Distance
N	Turn Ratio of Coil
R_L	Load Resistance
η	Efficiency
G	Distance Between Coils
I_{primary}	Current at the Transmitter stage
$I_{\text{secondary}}$	Current at the R stage
P_{in}	Input Power
P_{out}	Output Power
Resistance _{1,2}	Internal Resistance of Inductance
T	Length of the Coil
W	Width of the Coil

CHAPTER ONE

Introduction

1.1 Introduction

Wireless power transfer (WPT) is nowadays considered a very important topic due to many features. The common and main feature is that it can transmit power from the transmitter to the receiver device without using cables connecting them which means it is done through a gap. In recent years, WPT evolved significantly. So, it is considered the essential technique which can transmit power wirelessly and can be considered an important change to the traditional transmitting techniques that use cables [1-2].

WPT has many attractive features. Firstly, it is characterized by the ease of use in terms of reducing the use of wires. Secondly, WPT is safe, reliable, low in cost, and preserves the life of the device in terms of not needing to use cables. Thirdly, it protects the devices from heating or overcharging troubles. In addition, it is useful for the equipment of high cost charging [3-4]. This technology can transmit power for short and long distances for many applications, such as electric vehicles, portable devices, medical technology, and many others. WPT is divided into two types depending on the distance: the near-field type (can transmit power for short and medium distances) and far-field type (can transmit power for long distances) [1], [5-6].

There are two basic categories of WPT: coupling type and radiative type. These two types differ from each other in terms of the distance of transmitting power. The coupling type can transmit power for short and medium distances, whereas the radiative type can transmit power for far distances [7-8].

Any WPT system consists of two stages which are the transmitter and receiver. The devices used are the same for all WPT system but can differ depending on the type of application requirement or the parameter used, where some systems need to add an additional circuit to reach the appropriate results [9-10].

This thesis focuses only on the near field type WPT and the design in this study made for short or medium distances. The studies are still developing and discussing this topic to reach the best results.

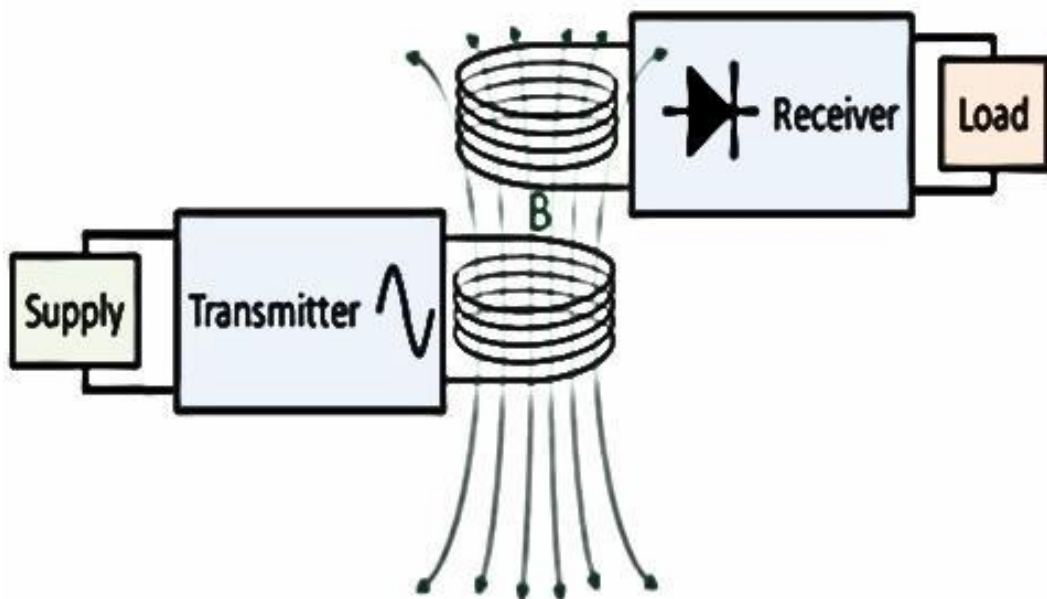


Figure 1.1 Work principle of WPT system [10].

Figure 1.1 illustrates the basic system and work principle of wireless power transfer technology, where each block will be discussed briefly in chapter 2. The B symbol represents the magnetic flux density between the transmitter and the receiver coil.

1.2 Comparison between wireless and wire charging.

There are many advantages of using wireless power transfer for charging devices. So, the following is an advantage of WPT that make it the preferable technique than wire charging [1],[19].

- In wireless charging, there is no need to use wires for charging which is reduce the complexity and saves the devices life.
- The safety and flexibility of wireless charging operation is more than wire charging.
- Efficient.
- It saves time and life device due to reducing using cables when charging.
- WPT is considered as one of the attractive technologies applications and can be developed to be more efficient than other devices.

1.3 Literature Review

The wireless power transfer technology is not new technique. It deals with the prediction that energy can be transmitted from one place to another through a gap as testified by Maxwell in his essay on Electricity and Magnetism since late 19th century [11].

In 2014, K. Aditya, introduced a comparison between series- series (S-S) and series- parallel (S-P) compensation circuit topology and concluded that the S-S topology has two features that make it better for use with inductive power transfer (IPT). The first is that primary capacitor is independent to the load or the magnetic coupling. The second is the secondary winding in the primary coil that has real reflected items. In addition, the S-P topology needs a controller for variable frequency which can add a complexity to the circuit where the S-S topology required

a fixed frequency. So, the S-S topology is the better topology for charging a battery for constant voltage and constant current charging [12].

In 2015 This paper proposed a novel DC-DC converter model based on the analysis of WPT and designed a feedback controller for the maximum efficiency control of WPT. Experimental results demonstrated that the analysis of the secondary current of WPT is acceptable, and that the maximum efficiency control through secondary voltage control is suitable for EV applications at any transmitting distance.

In 2016, A.T. Satel, designed a proposed system of wireless power transfer for charging a battery of laptop by 20V, 6A (120W). The number of turns of the coil is also discussed in this study and concluded that when the turn of the coil increased the coupling between coils increased. The result that has been obtained from the design and simulation indicates that can charging a battery of a laptop for the required specification is at efficiency equal to 62% [13].

In 2017 S. Luo, S. Li and H. Zhao. Proposed the optimal parameter design methods for four-coil, LCC and CLC structure. Then, the reactive power of the three optimized system using different compensation circuits is compared by analysis, simulation. And the results shows that the LCC compensation network has lower consumption of reactive power than CLC and four-coil structure, also when additional insulation is need, four-coil compensation would also be a good choice [7].

In 2017, Z. Liu et al. proposed a tank system for wireless power transfer that does not change a lot with the misalignment between the transmitter and receiver point. Also the efficiency of the system remains at the same value when the distance is changed from 30-100 mm between the transceiver points. The efficiency is equal to 71.77% for the measurement and simulation results to the success of the proposed system [14].

In 2018, Z. Zhang et al. presented an overview of WPT techniques with a concentration on the technical challenge and the applications. Then this study discussed the IPT system technique and concludes that the IPT of two coils can work only for short range distance applications where the IPT of four coils is used with higher distances [15].

In 2020, S. Kuka et al. present a review of the accomplishments of methods for increasing the efficiency and distance enhancement in WPT applications. The efficiency improvement depends on increasing the efficiency of all blocks that are included in the WPT system. Moreover, the efficiency of the system can be improved by: firstly, designing the coil correctly, secondly the compensation circuit of the resonance in the transceiver circuit, and other improvements that would be possible in the power converters topologies [16].

In 2021 Y. Zhang, S. Chen, X. Li and Y. Tang gives an overview of the state-of-the-art high-power static WPT systems via magnetic induction

In 2022, M. Amjad, et al discussed electric vehicle charging using the wireless power transfer technique. This study includes the importance of WPT technology, especially for electric vehicles which reduce or eliminate the wires and the mechanical connection between items. It also increases the system efficiency. The comparison between mutual coupling type, inductive and capacitive have been discussed to show the better technique for charging. Finally, the study reached that the inductive WPT is the appropriate method for wireless charging of electric vehicles [17].

1.4 Aims of the Thesis

The aim of this study is to design a WPT system for one of the modern technology which is the smartphone application. The following is the steps of discussed and designing the WPT system:

- 1- Recognizing the importance of WPT technology.
- 2- Designing a system to analyze the Frequency Splitting Phenomenon (FSP) before designing the WPT circuit.
- 3- Designing a WPT system using inductive power transfer type (IPT) with the resonance that can charge smartphone applications by (10W, 5V, 2A) at acceptable efficiency.

1.5 Thesis Outline

This thesis consists of four chapters organized as follows:

Chapter One presents an overview of the wireless power transfer (WPT) technology and discusses its type, in addition to the literature review and the aims of the study.

Chapter Two includes an introduction, and basic theories of WPT. It discusses briefly the types of WPT that had been used, explores the structure, and explains the way WPT operates and its applications.

Chapter Three includes the design and simulation results of the frequency splitting phenomenon and the wireless charging system of smartphone and discusses the effect of different parameters on the system performance.

Chapter Four includes the conclusions of the results that have been reached from this thesis study in addition to some suggestions for future work.

CHAPTER TWO

Basics of WPT System and their Applications

2.1 Introduction

Wireless power transfer (WPT) is considered nowadays an important technology due to many of its features. The main common feature between all types of WPT is that all methods transmit power using current (AC). Generally, transmitting power occurs by two methods: coupling and radiative [18-19]. The coupling method is classified into a magnetic field and electric field whilst the radiative method is classified into microwave and lasers. The magnetic and electric coupling types can transmit power at short and medium-range, this means it can be used for near-field applications whilst radiative is used in far-field type [20].

The working principle of WPT system is based on the magnetic flux generated between two coils at the resonance frequency, where these series capacitor values is chosen to suit resonance frequency [21]. The advantage of adding a series capacitor to form a resonator circuit is to obtain the maximum power transfer of the circuit. Moreover, some parameters can effect the power transfer such as, distance between coils, the appropriate frequency and so on [22-24].

Figure 2.1 shows the basic block diagram of wireless power transfer for the charging system.

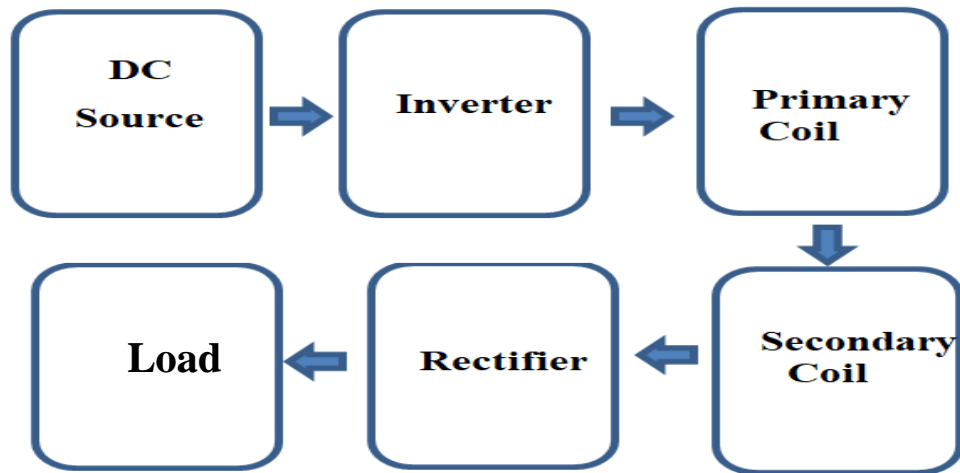


Figure 2.1 Typical diagram of WPT for charging the battery.

2.2 Applications of Wireless Power Transfer

Due to the advantages of WPT which are, safety, ease of use, and less complexity than other methods, wireless power transfer (WPT) technology has many applications. The most important applications of WPT are [25-28]:

1. Portable Devices:

The batteries of portable devices including, mobile phones, laptops, iPad, Air Pods, and a variety of modern smart applications can be charged by a wireless technique which can reduce the wires more than wire charging, which is the most important advantage in addition to many other advantages. This

2. Vehicle Charging:

Vehicle charging includes all kinds of electric cars, where charging a car wirelessly can save time. It can charge the car at home or at charging stations. There is static and dynamic charging, the dynamic charge is important but is still developing to reach the superior results.

3. Medical Equipment:

In medical equipment such as charged medical devices that are implanted inside the body, WPT can be used to eliminate the need for elicitation of the body.

4. Home Applications:

WPT can be used for home applications such as kitchen oven, kettle, blender, and so on, to avoid the electric shock, as any device can be charged by putting it on the charging place.

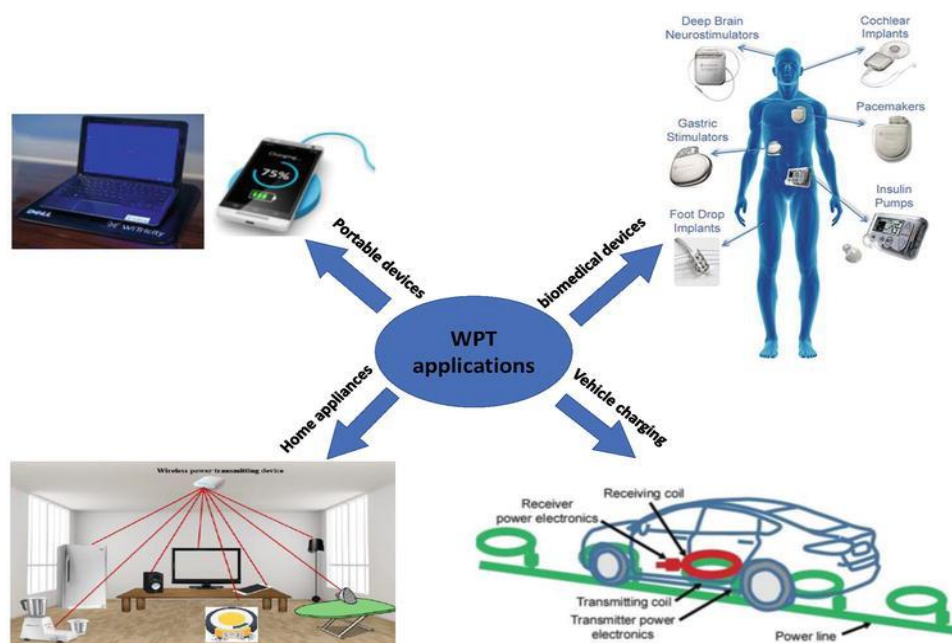


Figure 2.2 Wireless power transfer applications [25].

2.3 Wireless Power Transmission Types

Wireless power transmission WPT is a generic term that describes the various types of transmitting power wirelessly [29-31]. In general, there are two types of technologies that differ in range which could transfer the power to the load.

Figure 2.3 illustrates the types of wireless power transmission categorized into radiative and non radiative types.

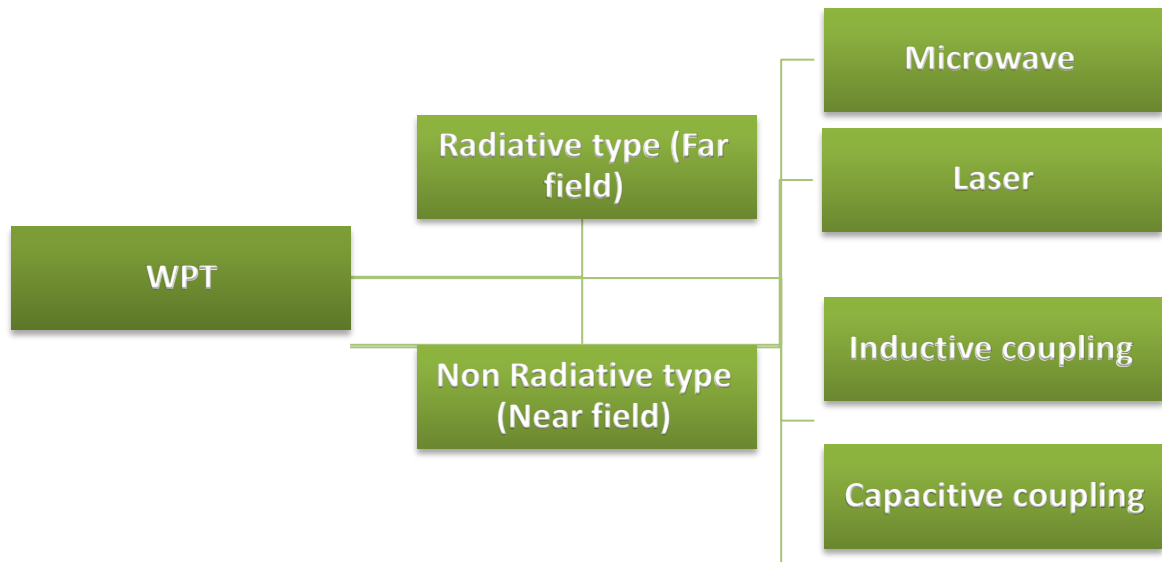


Fig. 2.3 Types of Wireless Power Transfer [29].

The main difference between the two types of the WPT near field and far field is the power transmission distance and the frequency, where the far field transfers power over medium and far distances with the range of frequency in GHz, for example, transmission using the laser or microwave is considered a type of far-field transmission. The near field is used for near distances of a few centimeters and the range of frequency is lower than far field transmission from KHz to MHz [32-33]. The near field type is higher efficient in power transmission than the far field type.

The power transmission depends on the distance between two objects. In the far field and near field, the power transmission is depends on the distance between coils [34-35]. Inductive coupling type was discussed in this thesis . Figure 2.4(a) shows the inductive coupling type and figure 2.4(b) shows the circuit of inductive coupling type after adding capacitance to the coils (L1, L2).

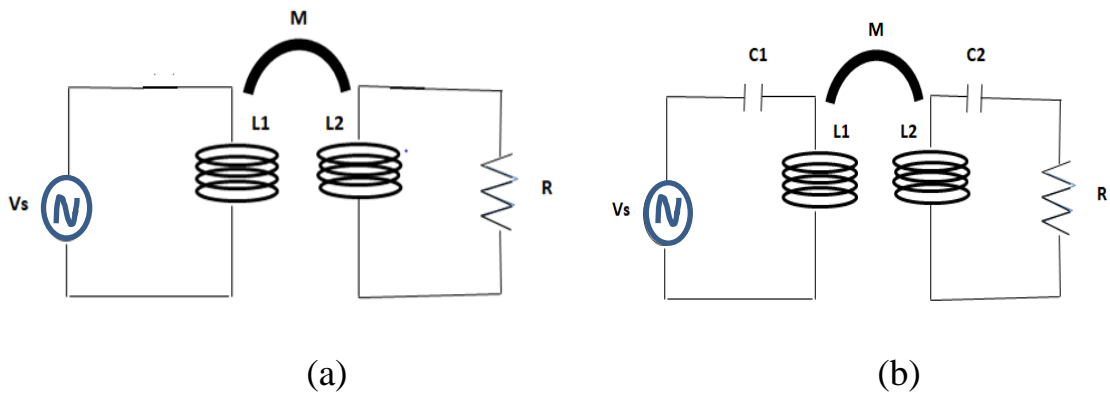


Figure 2.4 (a) Inductive coupling, (b) Resonance inductive coupling WPT System.

The inductive coupling system is termed resonance inductive coupling when adding a capacitance into one or two sides of the coils. There are four types of compensation circuits depending on the number and capacitance placed in the circuit. This circuit is termed compensation circuit[36-38]. The next section, gives more explanation about the compensation circuit.

1.6 Main Concepts of the Resonance Inductive Coupling Wireless Power Transfer System.

The main concepts of the WPT are discussed in the following sections.

1.6.1 Resonance

The resonance in the circuit that contains an inductor and capacitor is shown in figure 2.5. It occurs because the magnetic field of the inductor generates an electrical current in the winding that charges the capacitor. Then the capacitor discharging creates an electrical current that produces a magnetic field [39]. This process is repeated continuously which leads to creating the resonant frequency. At the resonant frequency in the series RLC circuit there are significant characteristics that can explain briefly. they are.

The capacitive reactance X_C and the inductive reactance X_L are equal.

- The total value of the impedance Z in the circuit will be minimum which is equal to resistance R .
- The current of the circuit will be the maximum value when the impedance is reduced.
- The voltage across the resistor equal to the supply voltage. Chapter Two 14
- The phase of the voltage and the current are the same making zero phase angle between them because the entire circuit is purely resistive and therefore the resultant reactance is zero.
- The power factor will be unity [42-44].

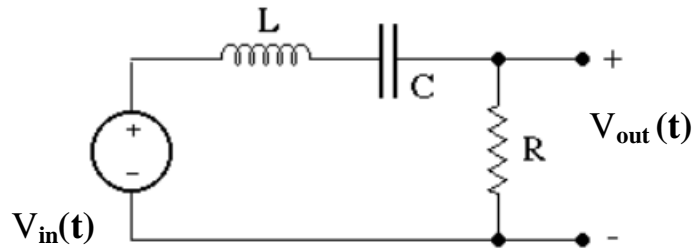


Figure 2.5 RLC series circuit[43].

The magnitude of the transfer function (TF) could be written as shown below when the output of the series circuit is taken across the resistor (R) [43].

$$\begin{aligned}
 |H(\omega)| &= \left| \left(\frac{V_{out}(\omega)}{V_{in}(\omega)} \right) \right| = \frac{R}{Z} = \frac{R}{\sqrt{R^2 + (\omega L - \frac{1}{\omega C})^2}} \\
 &= \frac{\omega * C * R}{\sqrt{\omega^2 * C^2 * R^2 + (\omega^2 * L * C - 1)^2}} \quad (2-1)
 \end{aligned}$$

$$|H(\omega)| = 1 \text{ correspond to } \omega^2 * L * C - 1 = 0 \text{ or } \omega_o = \frac{1}{\sqrt{L * C}}.$$

The resonance frequency depends on the coil and capacitor parameters. The maximum transmission of power can be obtained at the resonance frequency. The impedance of the RLC series circuit can be calculated as.

$$|Z| = \sqrt{R^2 + \left(\omega * L - \frac{1}{\omega * C}\right)^2}$$

At resonance condition, the inductive reactance ($X_L = \omega * L$) is equal to capacitive reactance ($X_C = 1 / \omega * C$). So, the impedance (Z) becomes pure resistive.

On both sides of the resonance maximum point, there are two points called the half power points because the power at these points is equal to half the power at resonance. At these points, the voltage across the resistance is reduced to $1/\sqrt{2}$ times the voltage at resonance. The frequency separation between these two frequency is called bandwidth (BW). So the transfer function could be written as:

$$\frac{1}{\sqrt{2}} = \frac{R}{\sqrt{R^2 + \left(\omega * L - \frac{1}{\omega * C}\right)^2}} \quad (2-3)$$

So the bandwidth can be calculated as shown below

By squaring Eq (2-3),

$$\frac{1}{2} = \frac{R^2}{R^2 + \left(\omega * L - \frac{1}{\omega * C}\right)^2} \quad (2-4)$$

The ω_1 , ω_2 are the roots that can be written as shown,

$$\omega_1 = -\frac{R}{2 * L} + \sqrt{\left(\frac{R}{2 * L}\right)^2 + \frac{1}{L * C}} \quad (2-5)$$

$$\omega_2 = \frac{R}{2 * L} + \sqrt{\left(\frac{R}{2 * L}\right)^2 + \frac{1}{L * C}} \quad (2-6)$$

So, the bandwidth equation is

$$BW = \omega_2 - \omega_1 = \frac{R}{L} \quad (2-7)$$

Where equation 2.7 can show the bandwidth is proportionate to the resistance **R**.

To find the resonance, multiply w_1, w_2 , where w is the angular frequency. (2-8)

$$w_0 = \sqrt{w_1 * w_2}$$

Where $w_0 = 2 * \pi * Fr$ so the resonance frequency (Fr) of the RLC series circuit is,

$$F_r = \frac{1}{2 * \pi * \sqrt{L * C}} \quad (2-9)$$

1.6.2 Quality factor (Q)

Quality factor (**Q**) is one of the important parameters that shows the capability of the inductor to save energy. The coil quality factor is inversely proportion to **R** (internal resistance of the coil) [45]. The internal resistance of the inductor means there is power consumption. Therefore, when the resistance value is small the quality factor of the coils becomes high and the efficiency is high. So, the quality factor is the ratio of energy stored in the system to the energy dissipated in the system [46].

Quality factor can be written as in Eq (2-10)

$$Q = \frac{\text{Energy stored in the circuit}}{\text{Energy dissipated in the circui}} \quad (2-10)$$

At resonant frequency, the quality factor can be written as

$$\text{Quality factor (Q)} = \frac{w_0 * L}{R} \quad (2-11)$$

Where $X_L = w_0 * L$, so

$$w_0 = 2 * \pi * Fr \quad (2-12)$$

1.6.3 Coupling Factor

Coupling factor is a measure of the amount of the interaction between two coils in a WPT circuit, where a higher coupling means there are small losses of the magnetic flux or there is high flux reaching to the receiver through the current generated and transferred from the primary to the secondary coil of the circuit. In addition, the coupling factor also depend on the distance between the coils. Whenever the distance between two coils is small the coupling become high, which means the losses in magnetic flux is small and the efficiency of the transmitting energy is high [46]. K is a unitless value and the values should be from 0 to 1. $K=0$, illustrate there is no magnetic flux reached to the receiver or the two coils not depend to each other. $K=1$ means there is a flux reaching to the receiver and it is considered as the perfect condition. The coupling factor can defined and calculated as the amount of magnetic flux that is transmitted from the transmitter coil to the receiver coil [47-49].

$$K = \frac{M}{\sqrt{L_1 L_2}} \quad (2-13)$$

1.6.4 Mutual Inductance (M)

When two resonant coils is placed close to each other, the magnetic flux in the primary coil tends to connect to the secondary coil and then induces a voltage in the secondary coil. So this operation of generating a current and voltage in the receiving coil is called the mutual inductance [44][50]. In addition, the distance can affect the mutual inductance value where whenever the distance between the two coils is small, the mutual inductance become high. To link the mutual inductance with the coupling factor, it can define the coupling factor is the amount of mutual inductance between the two coils [51][52] and the equation of mutual inductance can be written as shown below in Eq 2-14.

$$M = N_2 * \frac{\Phi_{12}}{I} \quad (2-14)$$

Figure 2.6 illustrates the conventional circuit of the resonant inductive coupling series capacitor.

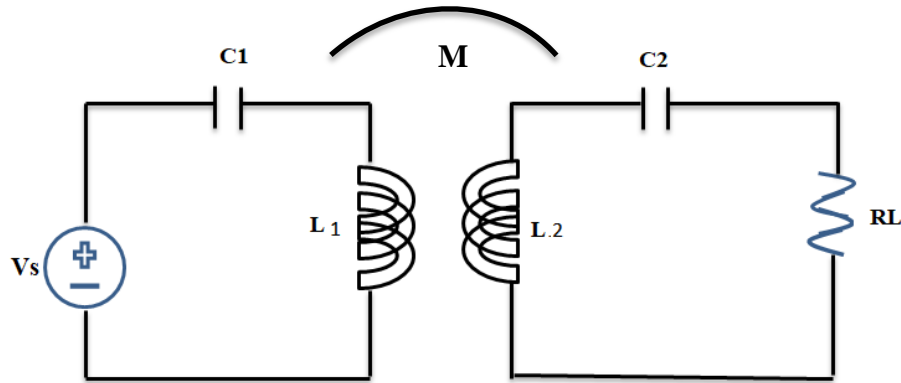


Figure 2.6 Conventional circuit of the resonant inductive coupling system

Where the V_s is the voltage source that generates the sinusoidal signal, C_1 , C_2 is the resonance capacitor of the coils L_1 , L_2 respectively. R_L is the load of the circuit, and M is mutual inductance.

1.7 The Components of Resonance inductive coupling power transfer (ICPT) System Achievement

Each system has a component that is considered a major element to enhance system performance. Resonance inductive coupling WPT consists of elements to form a WPT System, where each component can improve or can be chosen to suit the required system results.

Figure 2.7 shows the schematic diagram of the resonance inductive WPT system, to show the components arrangement of the system.

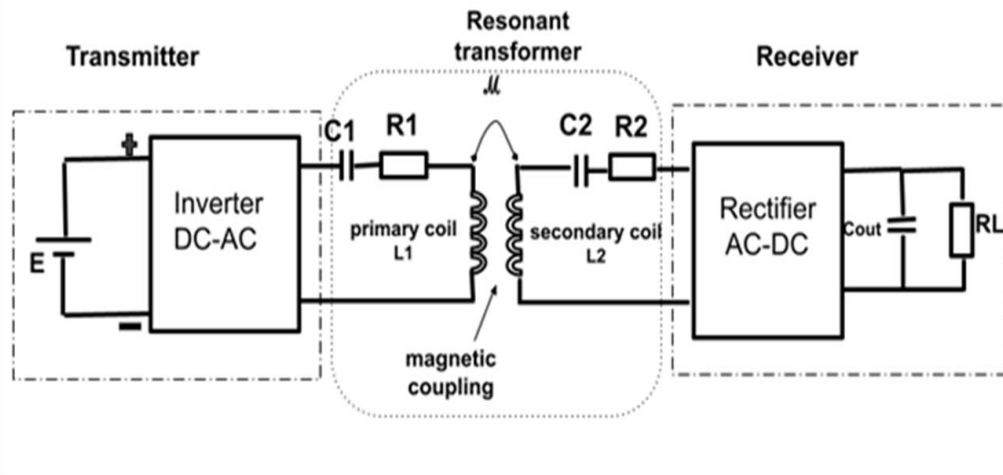


Figure 2.7 Schematic diagram of resonance inductive WPT system.

In the following sections, the major components of WPT system realization are discussed.

1.7.1 Compensation Circuit

Compensation circuit consists of C1 and C2 which are added to improve or increase the power transmitter efficiency of the system. these capacitors are added to the transmitter and receiver coils[53].

There are four types of compensation circuits according to the method of the capacitors linked with inductance or coils, which are series to series (S-S), series to parallel (S-P), parallel to series (P-S), and parallel to parallel (P-P). The S refers to the series connection and P refers to Parallel connection with the coil, so, the first character illustrates the method of the linked capacitor to transmitter side and the second character illustrates the method linking the capacitor to the receiver side. Figure 2.8 shows four types of compensation circuits [54-55].

The (S-S) type had been used in this thesis to design a WPT charging system because C1 behaves as a current source and produce a constant current that result to induce a voltage in the secondary coil. The C2 is to ensure the fixed resonance frequency independent of load and coupling and acts as voltage source that supplied a fixed voltage. So, the S-S topology is

the better topology for charging a battery for constant voltage and constant charging current and also for fixed frequency system[13].

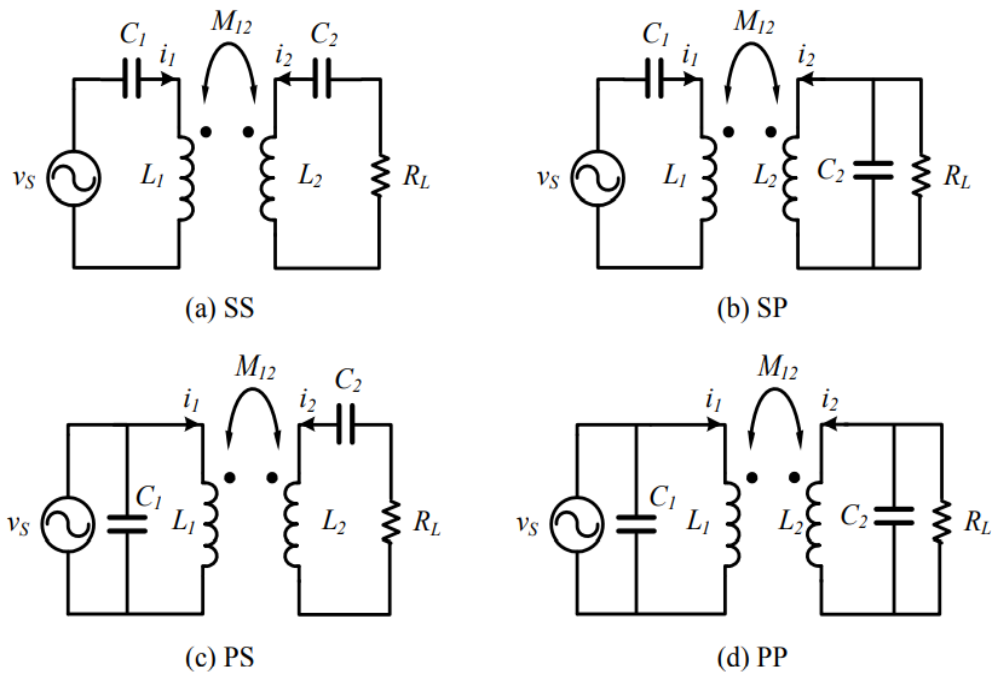


Figure 2.8 Compensation circuit types [55].

1.7.2 Inverter

The inverter is a device used to convert DC to AC signal, in the WPT system. The first component in the primary stage is the inverter which is supplied by the DC voltage source. Then this voltage is converted into an AC signal at the frequency which depending on the pulses applied on the gate[56]. After that, the generated AC current at the output of the inverter generates an AC alternating current flow in the secondary stage. There are two types of inverters to convert the DC to AC signal, half-bridge inverter and full-bridge inverter[56-59].

The following section includes a short discussion of the inverter types.

1.7.2.1 Half Bridge Inverter

Two power electronic switches are needed at the half bridge inverter which consists of IGBT or MOSFET, depending on the purpose that is needed. Also in half bridge type, the voltage is split into two 0.5 VDC of the full voltage and the voltage in the output is generated depending on the on-off switches of the MOSFET that is operated or determined depending on the frequency of the gate pulses. Figure 2.9 shows the circuit of the half-bridge inverter[57].

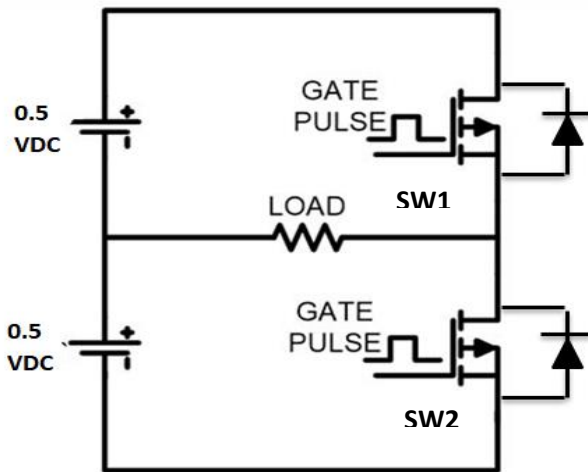


Figure 2.9 Half bridge inverter

Half-bridge inverter is operated with two modes, SW1, and SW2 the switches. So when SW1 is on the current path it flow from 0 to t_1 and SW2 is off as shown in figure 2.10.

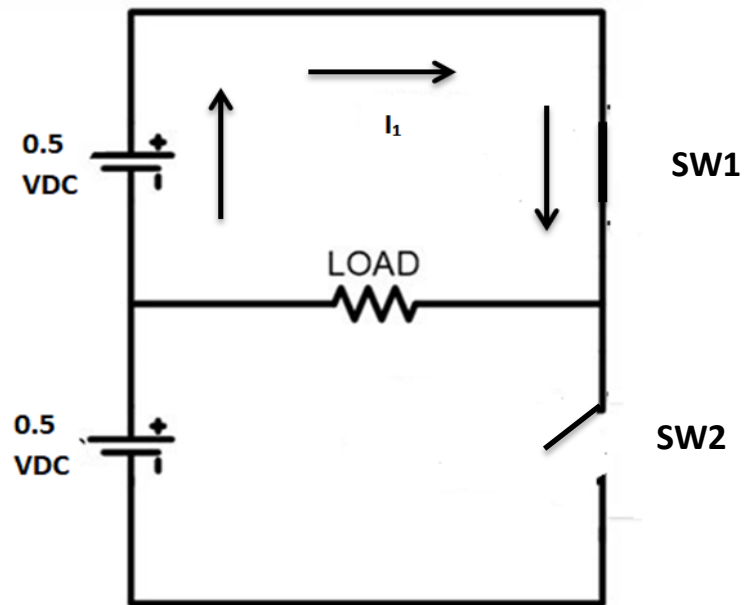


Figure 2.10 Current path at SW1= on, SW2 = off.

When SW2 is on, SW1 becomes off, and the current flows at half cycle from t_1 to t_2 as in figure 2.11.

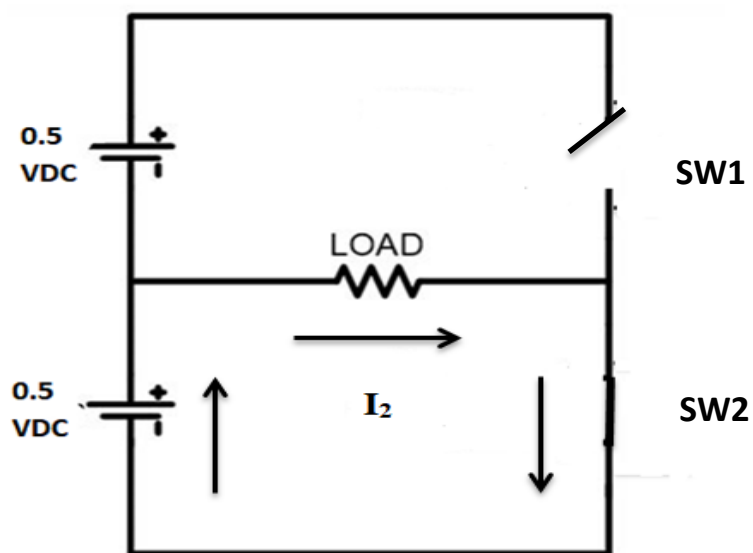


Figure 2.11 Current path at SW1= off, SW2 = on.

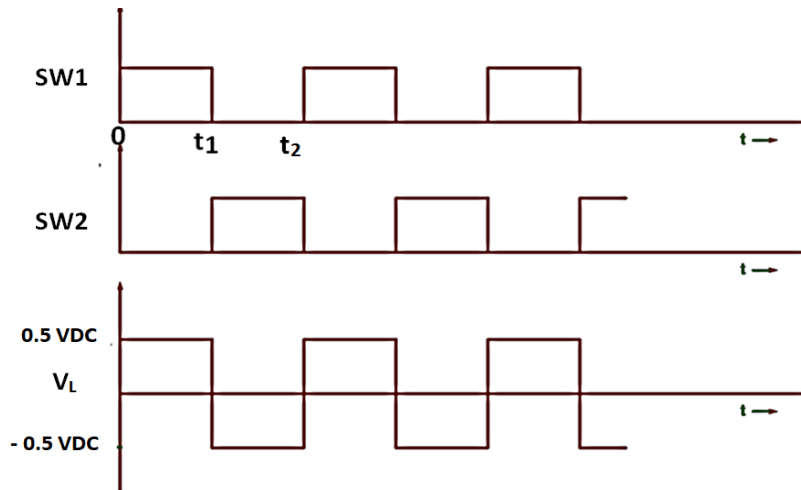


Figure 2.12 Output voltage V_L of half-bridge inverter at SW1, SW2.

Figure 2.12 shows the output voltage of the inverter where the output voltage is AC signal due to the current path from 0 to t_1 at SW1 and flows from t_1 to t_2 when SW2 is on [56-57].

1.7.2.2 Full Bridge Inverter

Full bridge inverter consists of four MOSFET or IGBT switches as shown in figure 2.13, and the voltage source is not split into two-parts. The operation mode and current flow through full bridge circuit are slightly different from the half bridge [57-58].

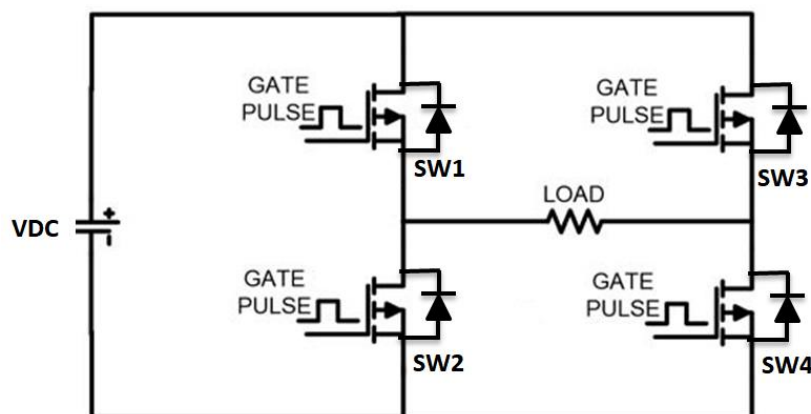


Figure 2.13 Full bridge inverter.

There are two modes of operation: the first mode is when SW1 and SW4 are on, so SW2 and SW3 are off. The current (I_1) flow through switches from 0 to t_1 as shown in figure 2.14.

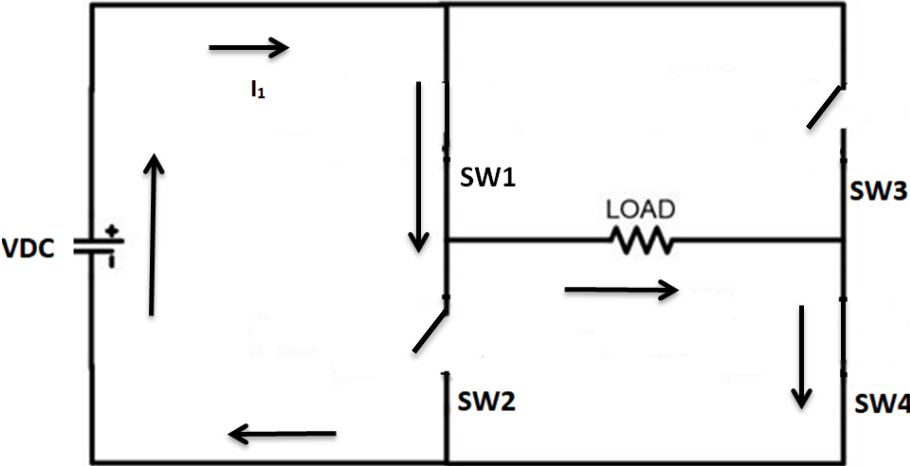


Figure 2.14 Current path at SW1 and SW4 on

The second mode is when SW2 and SW3 are on so, SW1, SW4 is off the current flow from t_1 to t_2 as shown in figure 2.15.

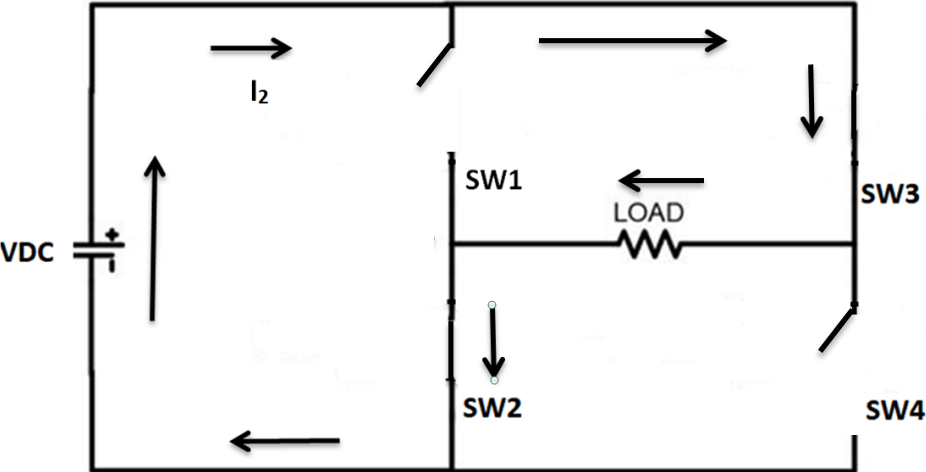


Figure 2.15 Current path at SW2 and SW3 on

The operation modes are not different from half bridge except that peak output voltage is VDC where peak load voltage is 0.5 VDC.

Figure 2.16 shows the load voltage of the full bridge inverter during the operation cycle.

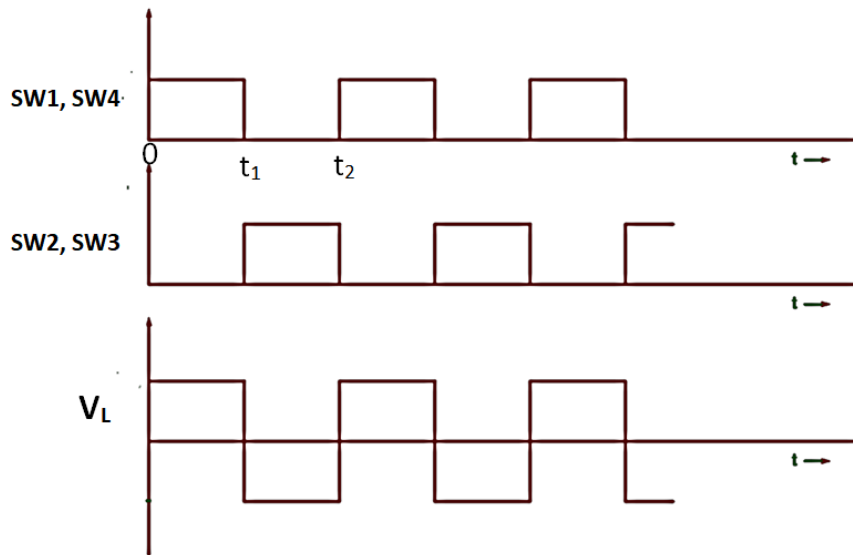


Figure 2.16 Output voltage VL of half-bridge inverter at SW1, SW2

The switching device that was used in this system is MOSFET, because MOSFET is suitable for low voltage operation, while an IGBT device is suitable for high current and voltage operation[13].

1.7.3 Rectifier

The rectifier is placed in the receiver stage before the load or the device that needs power because the rectifier is AC to DC converter. The signals of current and voltage received from coils are AC signals so the rectifier converts these signals into DC signals to be compatible with the load. In addition, a capacitor is linked with a rectifier as a filter to minimize the ripples of the signals[60-61].

Figure 2.17 shows the bridge diode rectifier. Where D1, D2, D3 and D4 are diodes, and the working principle is with two modes: the positive half cycle of the current flows through D1 and D2, and the negative half cycle of the current flows through D3, D4[62].

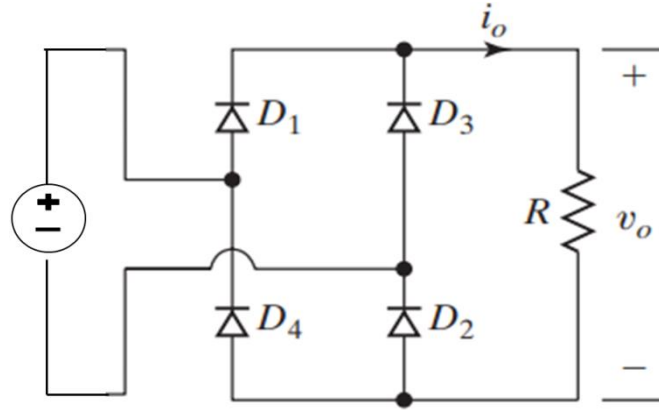


Figure 2.17 Full bridge rectifier[62].

1.7.4 Inductive Coils

The main component of any wireless power transfer system is the coil. There are two coils designed as the primary coil (L1) which is for the charger and the secondary coil (L2) is for a smartphone. The following equation is the theoretical parameter calculation to design coils and the analysis of the WPT equivalent circuit to calculate the efficiency of the system[63-65].

So L1 and L2 can be calculated as[64].

$$L1 = \frac{\mu_0}{\pi} * N1^2 * W * \log \left(2 * T1 * \frac{W}{R1 * (W + (\sqrt{T1^2 + W^2}))} \right) + \frac{\mu_0}{\pi} * N1^2 * \left(T1 * \log \left(2 * T1 * \frac{W}{R1 * (T1 + (\sqrt{T1^2 + W^2}))} \right) - 2 * (W + T1 - \sqrt{W^2 + T1^2}) \right) + \mu_0 * N1^2 * \frac{T1 + W}{4 * \pi} \quad (2-15)$$

$$L2 = \frac{\mu_0}{\pi} * N2^2 * W * \log \left(2 * T2 * \frac{W}{R2 * (T2 + (\sqrt{T2^2 + W^2}))} \right) + \frac{\mu_0}{\pi} * N2^2 * \left(T2 * \log \left(2 * T2 * \frac{W}{R2 * (T2 + (\sqrt{T2^2 + W^2}))} \right) - 2 * (W + T2 - (\sqrt{W^2 + T2^2})) \right) + \mu_0 * N2^2 * \frac{T2 + W}{4 * \pi} \quad (2-16)$$

Mutual inductance is important parameter for the system performance and we can notice from the equations that the mutual inductance depends on the physical dimension of the coils in addition to coupling factor also depending on the physical dimension and can be written as[65].

$$M = \left(\left(\frac{\mu_0}{\pi} \right) * N1 * N2 * T1 * \log \left(\frac{\text{sqrt}((G^2) + (W^2))}{G} \right) \right) \quad (2-17)$$

$$K = \frac{M}{\sqrt{L1 * L2}} \quad (2-18)$$

Where,

L1,L2: inductance

T1,T2: length of the coils

W: width of the coil

G: the distance between coils

μ_0 : permeability of the air = $4 * \pi * 10^{-7} \text{Hm}^{-1}$

M: Mutual inductance

K : Coupling factor

N1,N2: Turns ratio of the coils

R1, R2 is the radius of the windings

Each inductance has an internal resistance and can affect the efficiency. It is better to be small and can be calculated as shown below, where S1,S2 is cross section of the coils[64].

$$\text{Resistance 1} = \left(\left(\frac{1}{57} \right) * N1 * \left(\frac{2 * (T1 + W)}{S1} \right) \right) \quad (2-19)$$

$$\text{Resistance2} = \left(\left(\frac{1}{57} \right) * N2 * \left(\frac{2 * (T2 + W)}{S2} \right) \right) \quad (2-20)$$

The compensation elements C_1, C_2 should be chosen to achieve the same resonance frequency for the two stages. So, the resonance capacitance can be calculated as

$$C_1 = \frac{1}{\omega_0^2 L_1} \quad (2-21)$$

$$C_2 = \frac{1}{\omega_0^2 L_2} \quad (2-22)$$

Where the resonance frequency F_r can be calculated using Eq 2.9

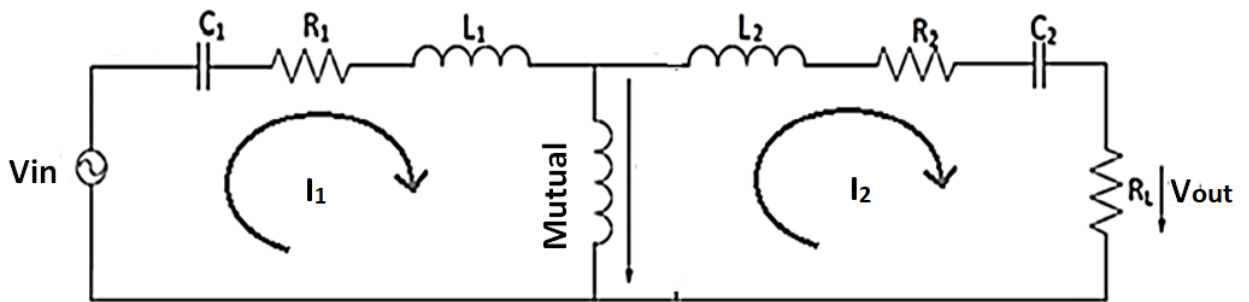


Figure 2.18 WPT equivalent circuit

The currents at the primary and secondary stages are shown in figure 2.18 and can be calculated in equation below

Where I_1 and I_2 is currents of primary and secondary stage respectively

$$I_{\text{primary}} = \frac{V_{\text{in}}}{Z_1} \quad (2-23)$$

Where Z_1, Z_2 stands for the impedance of the primary and secondary coil is

$$Z_1 = R_1 + j * \omega * L_1 + \frac{1}{j * \omega * C_1} + \frac{\omega^2 * M^2}{Z_2} \quad (2-24)$$

Where Z_2 is the impedance of the secondary stage and can be written as

$$Z_2 = R_2 + \frac{1}{j * \omega * C_2} + j * \omega * L_2 + R_L \quad (2-25)$$

So the current at the primary stage I_{primary} at resonance frequency can be written as

$$I_{\text{primary}} = \frac{V_{\text{in}}}{R_1 + \frac{\omega^2 * M^2}{R_2 + R_L}} \quad (2-26)$$

Where the current at the secondary stage (secondary coil) is generated by the induced voltage because the current variation at the primary coil can be written as

$$I_{\text{secondary}} = - \frac{j * \omega * M * V_{\text{in}}}{R_1 + \frac{\omega^2 * M^2}{R_2 + R_L}} \quad (2-27)$$

To observe the system performance and the efficiency that had been reached to achieve the required result, we should calculate the input power and output power as follows,

To find the power at the primary side P_1 and the power transmitted to the secondary coil P_2 (2-28)

$$P_1 = \frac{V_{\text{in}}^2}{Z_1} \quad (2-29)$$

$$P_2 = \frac{V_2^2}{R_L}$$

where V_2 is the voltage at the secondary side and R_L is the equivalent load resistance of the rectifier and the battery load. The efficiency can be calculated as in eq 2-30.

$$\text{PTE} = \frac{P_{\text{out}}}{P_{\text{in}}} \quad (2-30)$$

1.8 Smartphone Charging Work Principle

The principle of charging smartphones wirelessly is by placing the smartphone above the charger device across a small distance [68-69].

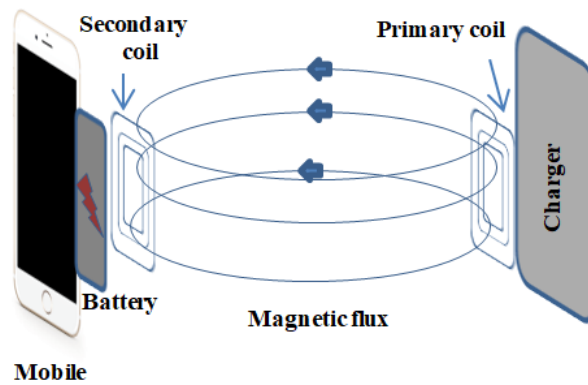


Figure 2.19 Work principle of wireless charging system.

Figure 2.19 clarifies the smartphone at charging operation. When placing the mobile on charger, an AC current flows through the primary coil causing a magnetic field that generating an AC current in the secondary coil. After that, this current is delivered to the battery as direct current by rectifier, which makes the battery charging[70-71].

From this principle can notice that there is no need to link the mobile to the charger by wires, for the safety, and flexibility of charging.

The following are the objects that should be in consideration when designing a WPT system for smartphone charging:

- The distance between two coils because it has an important effect on the system.
- Choosing the appropriate resonance frequency.

1.9 Frequency Splitting Phenomenon

Frequency splitting is a phenomenon that occurs in WPT system and can affect the system PTE. When the distance between two coils is decreased the PT and the efficiency is dropped sharply at the resonance frequency, while the resonance frequency is split in two new frequencies and the

power transmitter and efficiency become at maximum values at these two frequencies, this is called the frequency splitting. Figure 2.20 show the frequency splitting phenomenon at different distances[72][73].

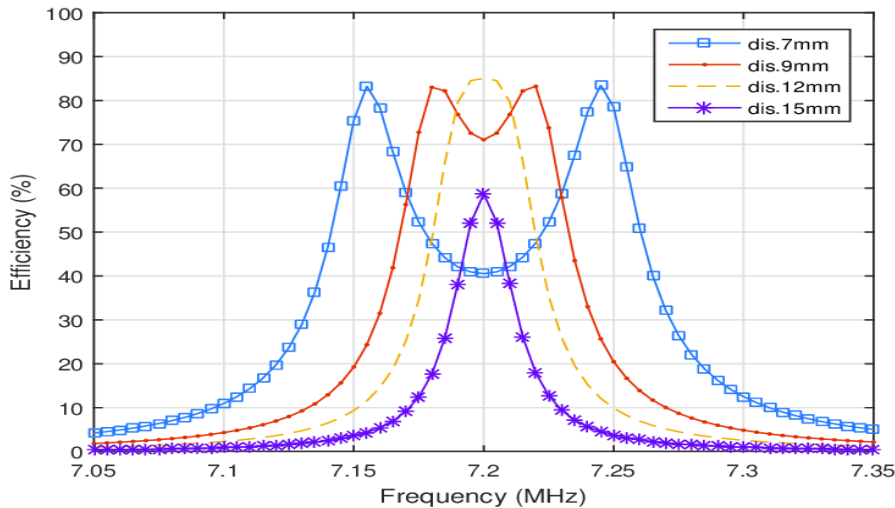


Figure 2.20 Frequency splitting phenomenon of two coils[68]

The relationship between the coupling factor and the distance is nonlinear. So, when the distance decreases, it causes the coupling factor to increase at the same time [45].

There are three situations of coupling:

- 1 Under Coupled range.
- 2 Critical Coupled range.
- 3 Over Coupled range.

In the under-coupled range the distance between two coils is large and the $K < K_{critical}$ which means the coupling between two circuits is low. Therefore the PTE and power transmission are small and on peak resonance frequency. This situation IS considered a non-efficient case.

The critical coupled range is considered the preferable situation where $K = K_{critical}$. In this case, the coupling between two coils is high, and the PT and

PTE are high at one peak of the resonance frequency. So the output of this circuit is considered an efficient signal.

When $K > K_{\text{critical}}$, this case is considered a non-preferable situation because the splitting in resonance frequency occurs, and when the coupling still increased, the splitting becomes higher and insecure. So, it can be noticed from figure 2.20 that critical coupling is at 12 mm and the PTE is at one peak resonance frequency.

CHAPTER THREE

Design and Simulation of the Wireless Power Transfer Using Resonance Technique

3.1 Introduction

In this chapter, the design and simulation results of the wireless power transfer circuit of smartphone charging by MATLAB program shows that, the results of the frequency changes can effect on the system efficiency or power transmission on the circuit. In addition, the effect of distance and resonance frequency on the system performance are simulated and discussed.

In recent years, the resonant inductive coupling (RIC) type of the WPT has become one of the most demanded technologies. WPT has a splitting frequency phenomenon (FSP). So, before designing the WPT technique system, a prototype has been designed by Advanced Design System(ADS) program and analyzed to show the effect of this phenomenon and the parameters that made this problem to be able to avoid this trouble when designing the system.

A compensation circuit designed and the (S-S) type has been chosen due to the importance of adding this compensation circuit which consists of (C1,C2) to improve the system performance.

WPT system has been designed, simulated and analyzed by MATLAB program. The WPT circuit consists of six stages: the input stage, Inverter device that used due to the DC input voltage, TX-RX coils that consist of the (L1,C1,L2,C2), rectifier device that used to convert the AC signals into DC signals and transmits these signals to the final stage which is called the load stage or the battery of the smartphones.

WPT can be extremely useful for many technologies used now for more ease of use [1-2]. The resonant frequencies that has been used in this thesis are from (50 KHz to 100 KHz).

In addition to discussing the parts of the circuits and their effect on the system performance, the purpose of this study is to design a coils and WPT that enable us to use in the field of charging application such as smartphones with 10W, 5V, and 2A with acceptable efficiency.

Figure 3.1 shows the arrangement of mobile charging system design and the technique of operation.

Figure 3.1 shows the technique of all elements arrangement where this technique represents the wireless smartphone charging. The charger can charge the devices that only have property of wireless charging which means the modern smartphones such as Samsung and iPhone with the new version.

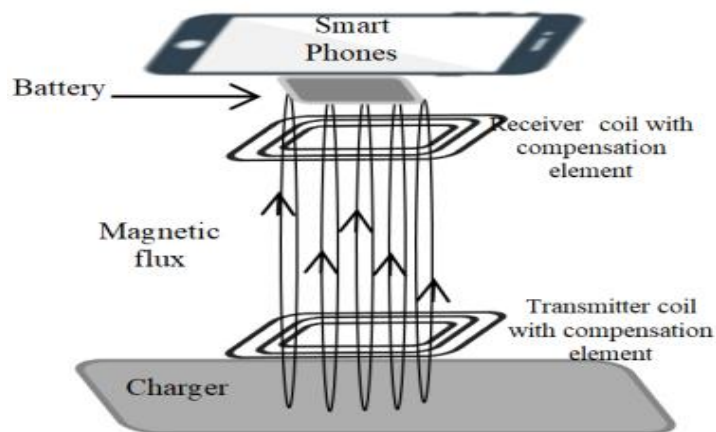


Figure 3.1 Smartphone charging operation technique.

Before explaining the system design of this thesis, it should demonstrate the problems that could be faced in the designing work. There is a problem in WPT which is frequency splitting phenomenon that should take into account when designing a WPT system. So firstly a prototype design is discussed to shows this problem. This design and Simulation is achieved by ADS program.

The required result is to obtain 10 W, with 5V and 2A to be suited for charging smartphones. The results are divided into the following sections.

- The result of a proposed system to clarify the FSP that is considered a problem in WPT and discuss the results.
- The result of a WPT proposed system to show the effect of frequency and distance changes on the system performance.
- Choosing the suitable parameters values for frequency and distance to obtain the better system performance.

3.2 Design and Simulation of the Proposed System of Frequency Splitting Phenomenon

The FSP is considered as a problem to some systems. So, in this thesis a small system has been designed and simulated by ADS Software to show this problem. Also from the figures (3.3-3.10) can be observed the effect of some parameters on the efficiency and the system performance.

Figure 3.2 is a prototype of WPT system which consists of two coils and two capacitor to represent the design of WPT system used to clarify frequency splitting phenomenon.

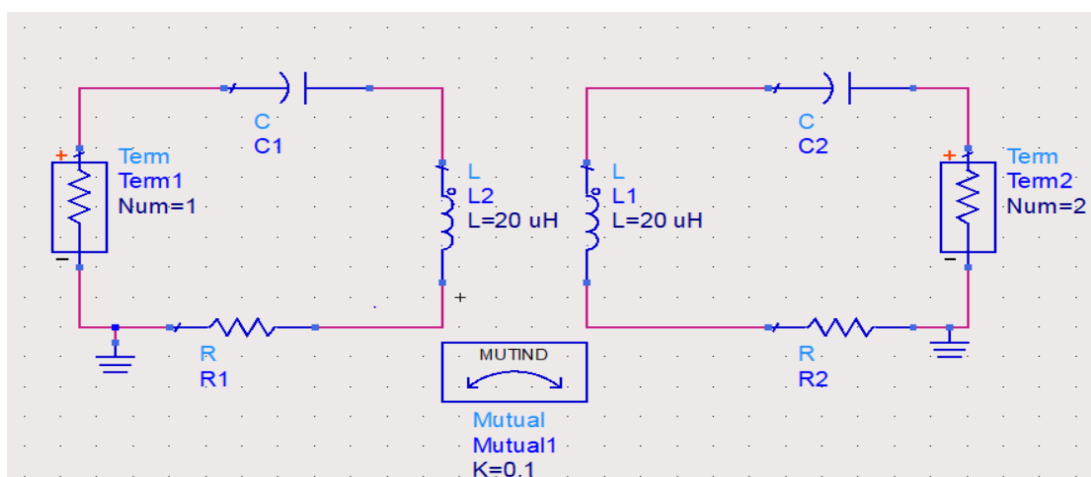


Figure 3.2 Topology of WPT for FSP design.

The amount of power transmission from the source to the load is depends on the matching between the source and load so when matching occur the power is transmitted to the load. The maximum power transmitter efficiency can be obtained at the optimal frequency when coupling factor K at critical value.

Where

R_1, R_2 internal resistance of the primary and secondary inductance.

K : Coupling factor.

K have three situations: under coupling, critical coupling and the over coupling.

Critical coupling is the appropriate situation where the PTE become at maximum values whilst at over coupling situation. The PTE becomes at lower value at the optimal frequency and at high value at the two new sided frequency which called the frequency splitting phenomenon.

The main parameters that affect the system performance and should be in consideration when designing a system are:

- Coupling coefficient k : The effect of coupling to compare and show the effect on the system at each frequency .
- The distance where there is a nonlinear relation between distance and k .
- Resonance frequency (f_r): The FSP occurs at higher distances when frequency increasing

4.1 Simulation Results of the Frequency Splitting Phenomenon (FSP).

In this section, the results of FSP designing circuit had been shown and discussed in figure 3.1, The ADS program is used to simulate the circuit. The parameters of the design are proposed in this circuit to exhibit the comparison between three frequencies (10, 20, and 30 MHz) on the wireless power transfer system

3.2.1 Simulation Results of the Frequency Splitting Phenomenon at Fr=10 MHz.

The equation used by (ADS) program to show the Efficiency curve is shown below. Where S21 is s-parameter.

$$Eff = 100 * ((magS21) * mag(S21)) \dots \dots \dots (3 - 1)$$

Where
 R1,R2 =0.5 Ω
 C1,C2=12.67 PF

Figure 3.3 shows that the efficiency is approximately 62 % at a resonance frequency equals to 10 MHz, and coupling factor equals to 0.02 at under coupled situation which is one of the three situations of FSP discussed in chapter 2.

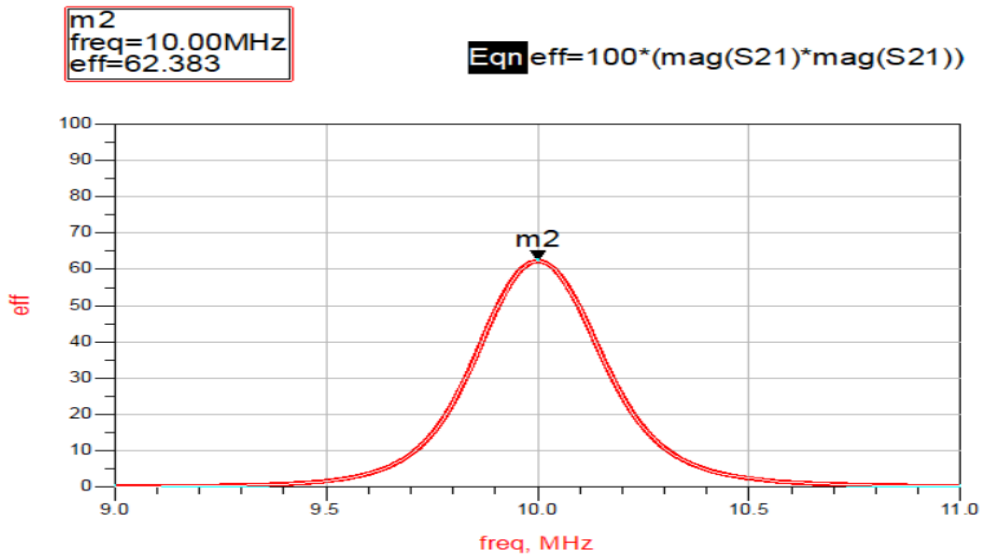


Figure 3.3 Efficiency for under coupled range at K=0.02, Fr=10 MHz.

It can be noted from figure 3.4, the increase in the efficiency of the power transmitter in critical coupled situations is equal to 98 % at K = 0.04, Fr =10 MHz. where K is the coupling factor, and Fr is the resonance frequency.

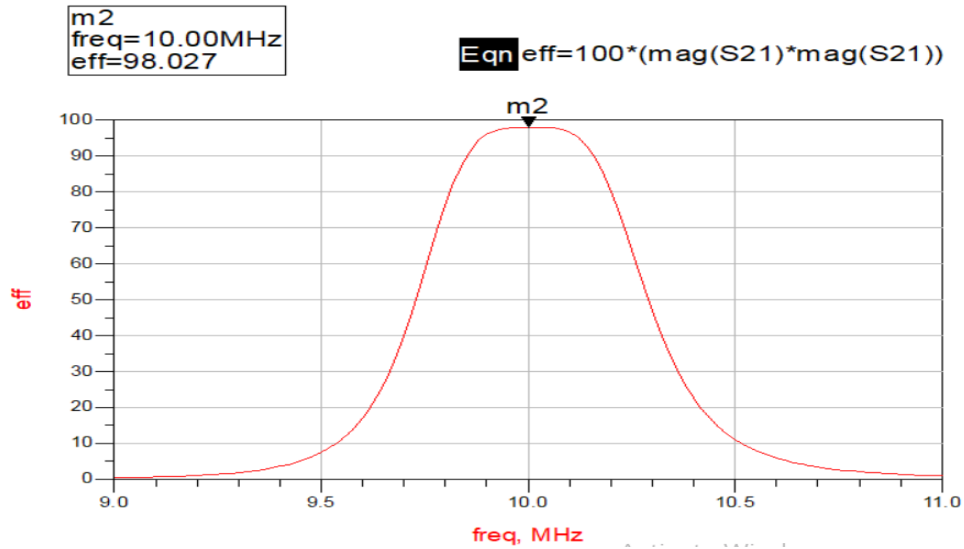


Figure 3.4 Efficiency for critical coupled range at $K=0.04$, $F_r=10$ MHz.

It is noted from figure 3.5 that there is a drop in efficiency at the resonance frequency, where it is equal to 93 % as shown in figure 4.5 and the higher value at the two new-sided frequencies 9.5 and 10.5 MHz.

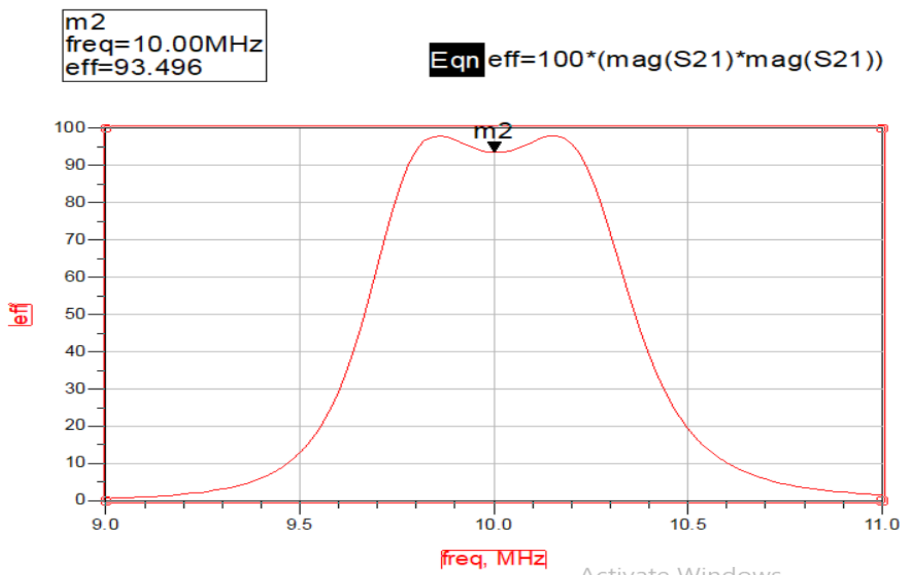


Figure 3.5 Efficiency for over coupled range at $K=0.05$, $F_r=10$ MHz.

Figures 3.3, 3.4 and 3.5 show the three situations of coupling and can be noted the high effect of coupling coefficient changing in values on the power transmitted efficiency (PTE). The efficiency becomes at lower values at under coupled range where better PTE is at critical coupled value,

and the splitting in frequency and power sharpened at over coupled range which is considered the worst situation for the system because the power transmitted is becomes at lower values.

Table 3.1 shows the summarized results at $F_r=10$ MHz of maximum efficiency values at coupling factor values including under coupled, over-coupled, and critical coupled.

Table 3.1 Maximum efficiency at three coupling situation at $F_r=10$ MHz.

Situation	Coupling Coefficient (K)	Max Efficiency(η)%	Frequency
Under coupled	0.02	62	10 MHz
Under coupled	0.03	90	10 MHz
Critical coupled	0.04	98	10 MHz
Over coupled (FSP)	0.05	97	8.18 MHz
		98	14.14 MHz
Over coupled	0.07	97.8	18.42 MHz
		98	7.66 MHz

From Table 3.1 can be noticed, that at under coupled range when $K = 0.03$ the maximum efficiency is 90%, and when K is decreased to 0.02, the maximum efficiency is 63%, where the coupling at this situation is weak so the system efficiency is decreased. At the critical coupled range when $k=0.04$, the maximum efficiency is 98%. The over coupled range is from above $K= 0.04$ to 1 where the maximum efficiency is at two new sided frequency.

3.2.2 Simulation Results of the FSP at $F_r= 20$ MHz.

In this section the three situation of FSP had been shown to compare between the situations of the previous section at $F_r=20$ MHz.

Where
 $R_1, R_2 = 0.5 \Omega$
 $C_1, C_2 = 3.16 \text{ PF}$

Figure 3.6 show the critical coupled situation where the efficiency is at the higher value at $F_r = 20 \text{ MHz}$ equal to 98 %.

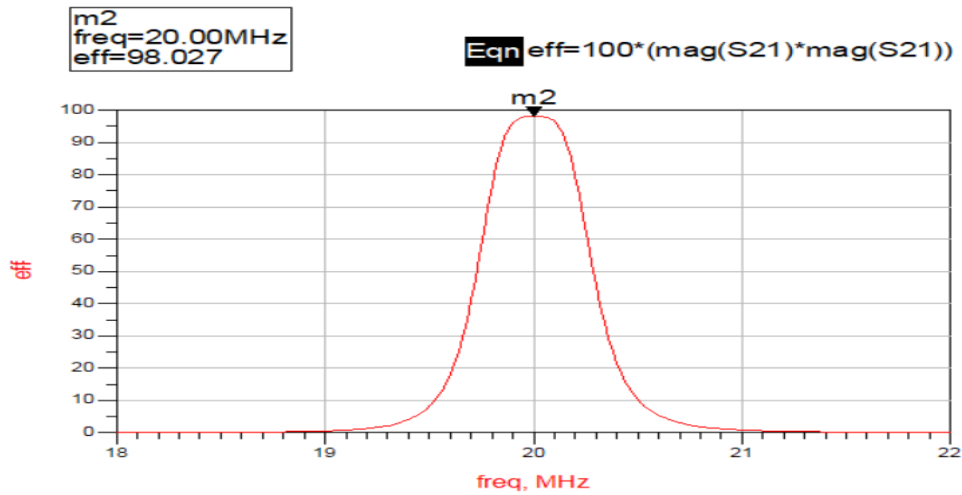


Figure 3.6 Efficiency for critical coupled range at $K=0.02$, $F_r=20 \text{ MHz}$.

Figure 3.7 can show the over coupled situation where the splitting occurs that make efficiency approximately 85 % at resonance frequency whereas the higher frequency is at two new sided of resonance frequency at $F=19.7$ and 20.3 MHz .

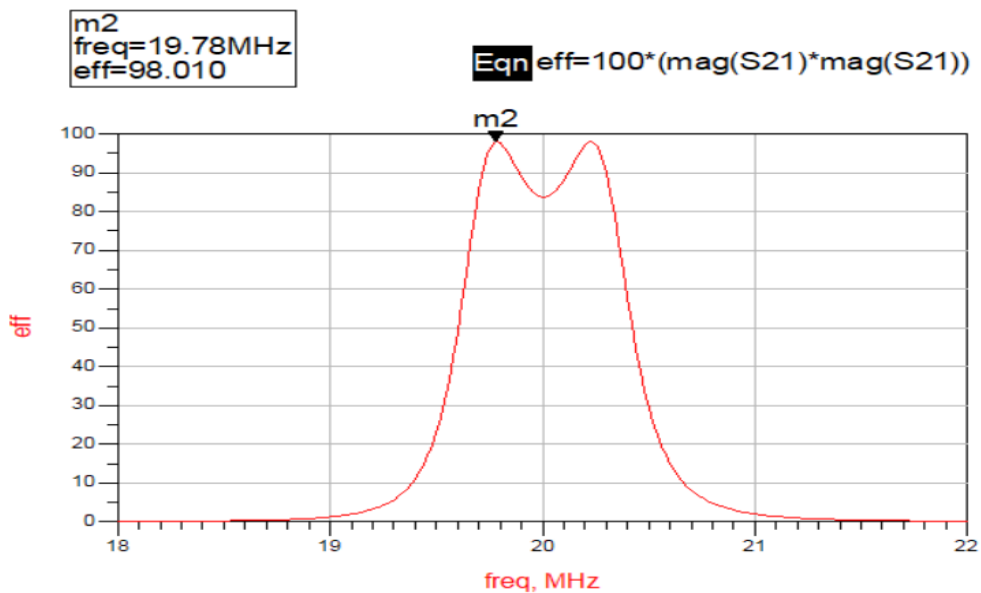


Figure 3.7 Efficiency for over coupled range at $K=0.03$, $F_r=20 \text{ MHz}$.

Table 3.2 shows the summary of three situations at $F_r=20$ MHz. where it notice that the critical couples at $K= 0.02$ and the splitting becomes at $K=0.03$, whilst the splitting occur at $F_r= 10$ MHz at $K=0.05$, which it meant the splitting in frequency occur at $F_r= 20$ MHz at coupling value lower than $F_r=10$ MHz.

Table 3.2 Maximum efficiency at three coupling situation at $F_r= 20$ MHz.

Situations	Coupling Coefficient (K)	Max Efficiency(n) %	Frequency
Under coupled	0.01	62.38	20 MHz
Critical coupled	0.02	98	20 MHz
Over coupled	0.03	98	19.78 MHz
		97.9	20.24 MHz
Over coupled	0.5	97.8	16.34 MHz
		98	28.8 MHz

3.2.3 Simulation Results of the Frequency Splitting Phenomenon at $F_r= 30$ MHz.

In this section also the situation had been shown to compare the results between the three sections to know the effect of frequency increase on the system and when the splitting occur.

Where $R_1, R_2 = 0.5 \Omega$

$C_1, C_2 = 1.41$ PF

It can be noted from figure 4.8 that the efficiency is equal to 97.9 % at $K=0.013$ for critical damp range which arrives to critical value at a lower coupling coefficient value compared to the two sections of $F_r=10$ and 20 MHz.

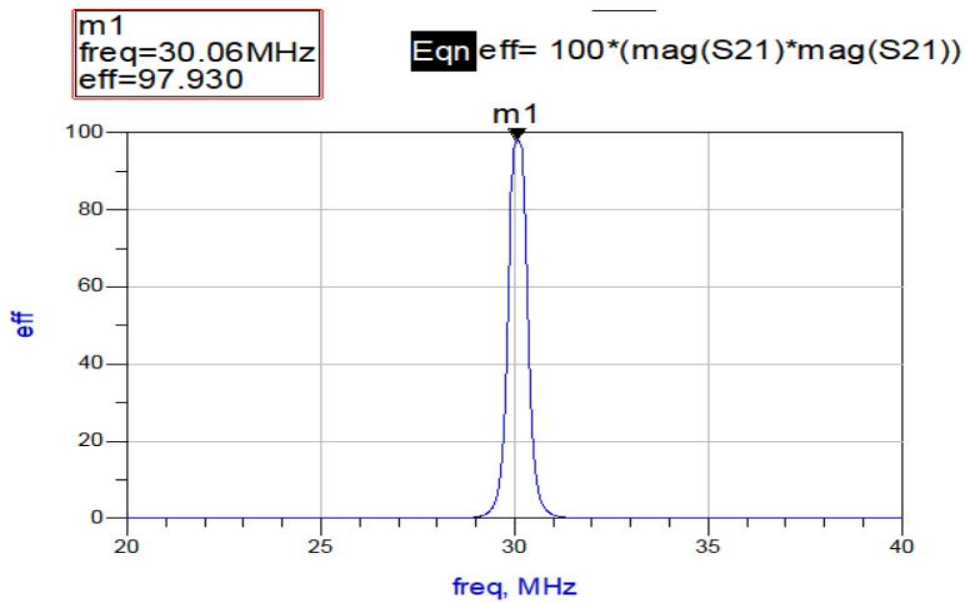


Figure 3.8 Efficiency for critical coupled range at $K=0.013$, $Fr=30$ MHz.

Figure 3.9 shows the splitting in frequency that occurred at $K= 0.02$ and the power transmitter efficiency dropped to 86 % where the high efficiency at the two new frequencies where $Fr= 29.8$ and 30.4 MHz = 98 and 97.7 respectively.

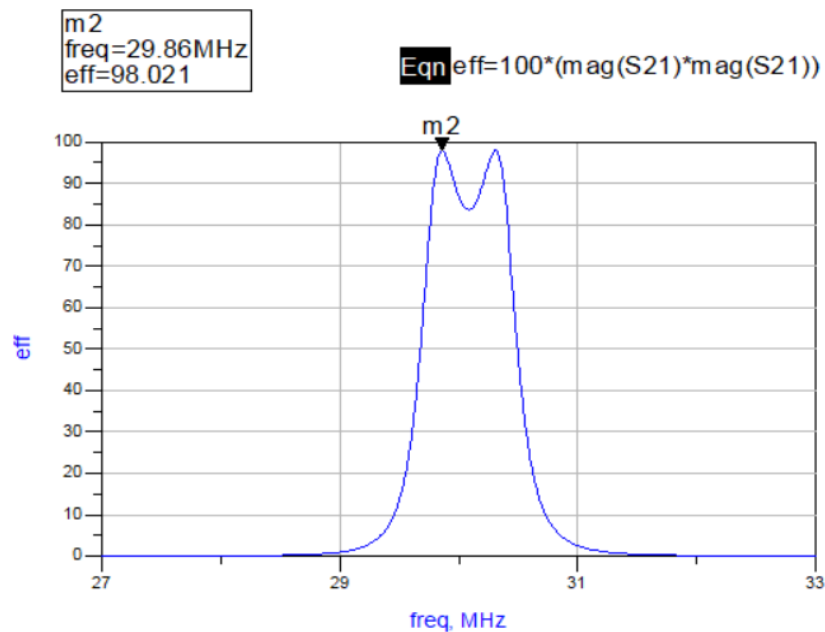


Figure 3.9 Efficiency for over coupled range at $K= 0.02$, $Fr= 30$ MHz.

It can be noticed from Table 3.3 that the under coupled range becomes $K=0.01$ and max efficiency= 90 where the critical coupled range is at 0.013 and the max frequency is = 98, and the over coupled starts from 0.013 to 1. The over coupled starts from a lower value of K than the other cases listed above which are at $F_r=10$ MHz and 20 MHz and this effect increases efficiency, figure 3.10 summarizes the results of the three cases briefly.

Table 3.3 Maximum efficiency at three coupling situations at $F_r=30$ MHz.

Situations	Coupling Coefficient (K)	Max Efficiency(n)%	Frequency
Under coupled	0.01	90	30 MHz
Critical coupled	0.013	98	30 MHz
Over coupled	0.02	98	29.86 MHz
		97.7	30 MHz
Over coupled	0.03	98	29.68 MHz
		97	30.48 MHz
Over coupled	0.4	97.9	25.4 MHz
		98	38.8 MHz

4.4 Comparison Results among three Frequencies 10, 20 and 30 MHz.

To clarify the results of the three sections and compare them, the frequency splitting phenomenon and the effect of this phenomenon on the system must be clarified.

It can be noted from figure 3.10 that the coupling coefficient at three frequencies: at $F_r= 10$ MHz the splitting in Frequency occurs at $K=0.05$, and when $F_r=20$ MHz the splitting in frequency occurs at $K= 0.03$, and at $F_r= 30$ MHz the drop of efficiency and splitting frequency occurs at $K= 0.02$.

In brief this result means, whenever the frequency of the system increases, the splitting in frequency will occur at lower K.

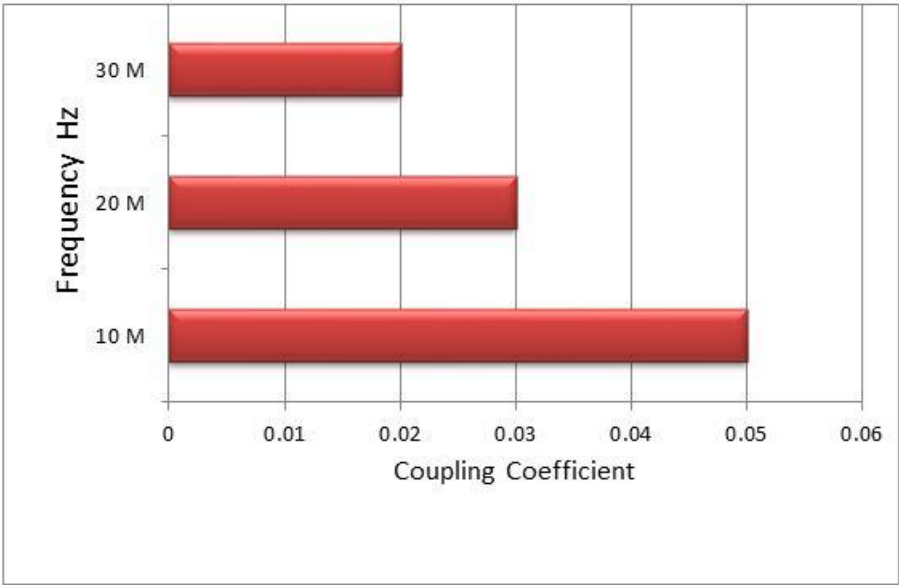


Figure 3.10 The splitting in frequency among 10, 20 and 30MHz.

The results shows the effect of the changing frequency on the system performance which leads to an effect on the system efficiency. Increasing and decreasing in frequency can affect the system performance. Therefore, when designing a WPT system, the choice of appropriate frequency of the circuit should be considered. The impact of splitting frequency on the system is when the frequency increases, which leads to the appearing of the FSP at a lower coupling coefficient than higher frequencies. This means that the critical coupling value of the system does not depend just on the circuit parameter but on the frequency of the system.

3.3 Coils Parameter Design of WPT Charging System.

The selection of coils parameter had been chosen depending on familiar smartphones dimension to be compatible with them Table 3.1 shows the parameters that had been used to design coils for WPT system. Figure 3.3 illustrates the dimensions of the coils, one of the coils is for the charger device and the other is for the smartphone device. The transmitter and receiver coil that have been injected into the charger and the receiver such as smartphone is shown in figure 3.2 which it is parameter designed in this study by MATLAB program.

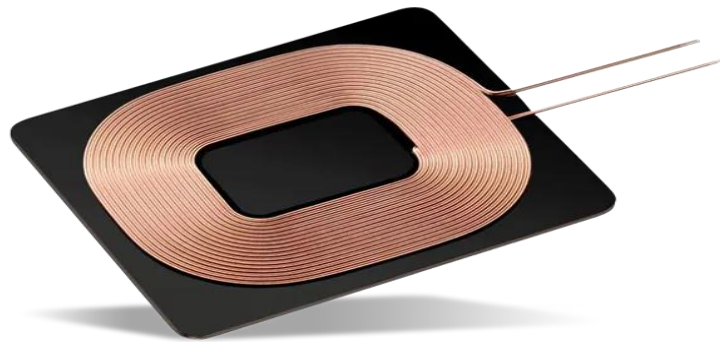


Figure 3.11 Coil for wireless charging.

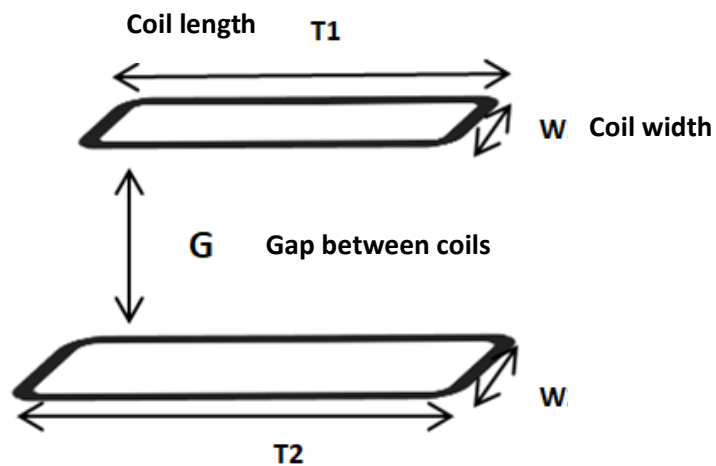


Figure 3.12 Diagram illustrates the notations used for the coils design.

Table 3.4 Parameters of the Smartphone Charging System Coils.

Parameters	Values
TX, RX coil length (T1,T2)	200mm, 185mm
Coils width (W)	60mm
Number of turns (N1,N2)	12,12 turns
The gap between coils (G)	30 mm

3.2.1 Circuit Parameter Calculation

To get the values of inductance by calculations for the coil that had been designed, the expressions described below can be used.

% Find L1 L2

L1

$$= u_0/\pi * N_1^2 * W * \log(2 * T_1 * W / (R_1 * (W + \sqrt{T_1^2 + W^2}))) + u_0/\pi * N_1^2 * (T_1 * \log(2 * T_1 * W / (R_1 * (T_1 + \sqrt{T_1^2 + W^2})))) - 2 * (W + T_1 - \sqrt{W^2 + T_1^2}) + u_0 * N_1^2 * (T_1 + W) / (4 * \pi);$$

L2

$$= u_0/\pi * N_2^2 * W * \log(2 * T_2 * W / (R_2 * (W + \sqrt{T_2^2 + W^2}))) + u_0/\pi * N_2^2 * (T_2 * \log(2 * T_2 * W / (R_2 * (T_2 + \sqrt{T_2^2 + W^2})))) - 2 * (W + T_2 - \sqrt{W^2 + T_2^2}) + u_0 * N_2^2 * (T_2 + W) / (4 * \pi)$$

```

% Mutual inductance
M1=((u0/pi)*N1*N2*a*log(sqrt((G^2)+(W^2))/G));

```

The resistive values of coil windings can be calculated by:

```

% Find Resistance of the coils Res1 and Res2
Res1=((1/57)*N1*((2*(T1+W))/S1)); % resistive value of the windings
Res2=((1/57)*N2*((2*(T2+W))/S2)); % resistive value of the windings

```

Where

S1,S2: is the cross section of the coils

R1,R2 :Radius of coils windings.

W :Coils width

T1,T2: Coils length.

μ_0 : Permeability of the air $=4\pi*10^{-7}$.

N1,N2: Turn ratio

3.2.2 Resonance Frequency Calculation Code:

To get high power efficiency, the operation frequency should be at resonance, which leads to reducing the reactance.

$$Fr = \frac{1}{2*\pi*\sqrt{L.C}} \quad (3-1)$$

```

% Second way to calculate the resonance frequency

```

```

wo=(1/sqrt(L1*C1));

```

Where the C1, C2 must be chosen to be compatible with resonance frequency of the transmitter and receiver coil to achieve a good matching and the maximum power transfer efficiency.

```

% Find C1 and C2
C1=1/((2*pi*f)^2*L1); % Capacitor 1
C2=1/((2*pi*f)^2*L2); % Capacitor 2

```

Where f_r : Resonance frequency

C_1, C_2 : Capacitance of the primary and secondary coil

L_1, L_2 : Inductance of the primary and secondary coil.

ω_0 is angular frequency = $2 \cdot \pi \cdot f_r$.

3.3 WPT Proposed Design of Smartphone Charging Application

Fig 3.13 shown the full structure design of WPT in MATLAB Simulation where all the stages discussed above in details. The transmitter stage is considered the charger and the receiver is the device such as smartphones which is the device discussed in this thesis. This system works in the form of transmitting the DC voltage to the load or smartphones to charge the battery of load by $V_{DC}=5V$, $I_{DC}=2A$, $P(\text{power})=10W$.

The first step of the system is to supply a DC voltage from the source. After that the inverter (DC-AC) is located on the first stage at the primary side of the system which is supplied by the DC voltage from the source to generate the AC voltage and current. After that an AC current is induced in the primary coil which cause flowing an AC current in the secondary coil. Then the AC current and voltage in the secondary side is converted into DC current and voltage by the rectifier (full bridge) which exists before the load where the capacitance in the load is for smoothing DC signal,

Finally the DC current and voltage is transmitted to the load or the smartphones to supply the device with a power to be charging.

This system operation is to transmit power when Dc voltage is supplied.

The familiar parameters that can effect on WPT system and hinder performance or efficiency of the system are:

- Distance.
- Frequency.
- Inductance and capacitance values.

These parameters that affect the system are explained to clarify the effect of each one on the system performance to choose the appropriate values. In the next chapter the results and comparisons of the thesis parameters effect are shown.

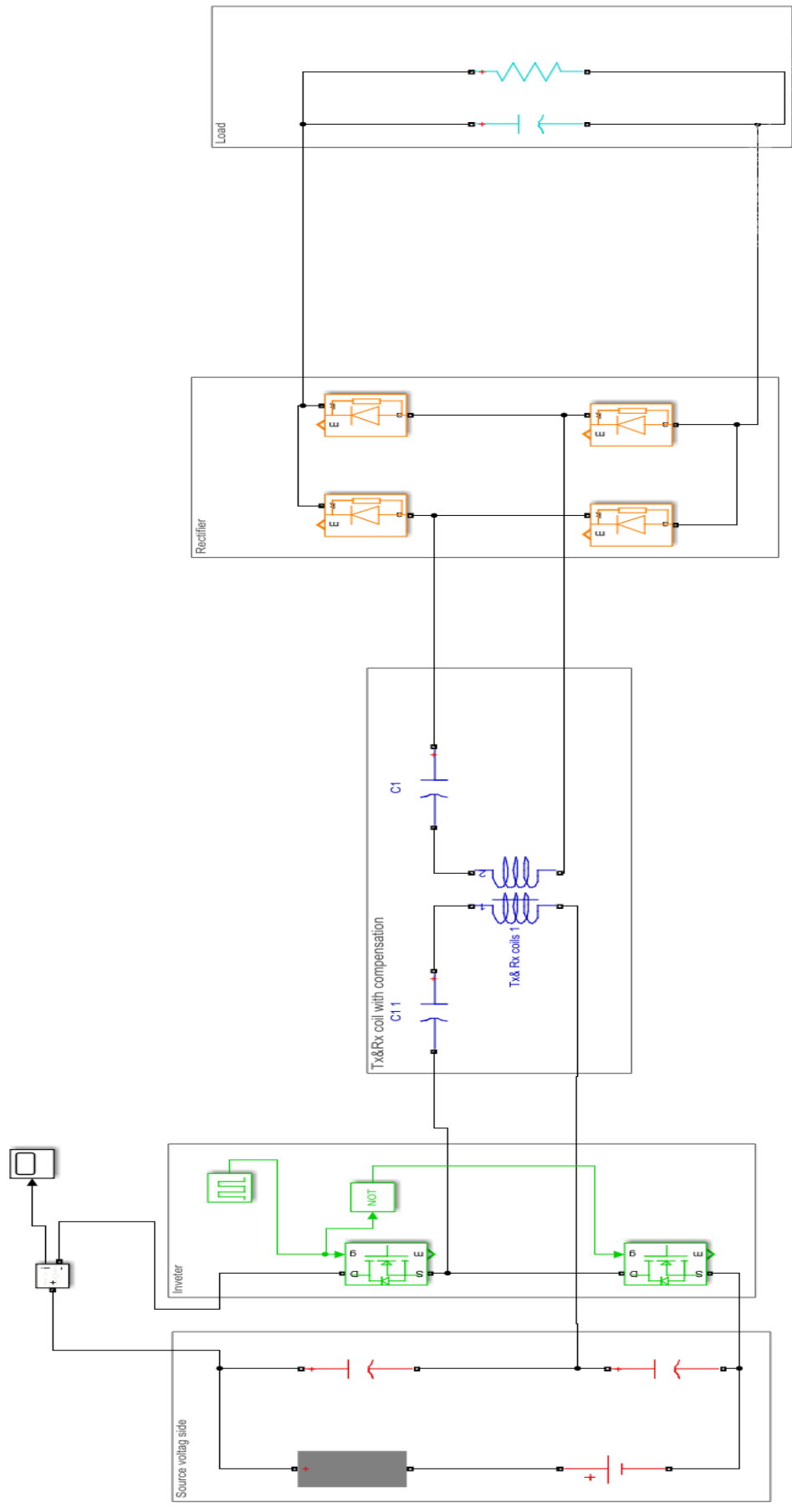


Figure 3.13 Proposed design of smartphone charging applications

A WPT system which is composed of two stages, transmitter and receiver is designed and simulated by MATLAB program with various frequencies and distances because of the importance of this parameter in improving the efficiency of the circuit. The first stage consists of Dc source and inverter to convert the DC signals into AC signals to move through Tx coil.

The receiver side consists of a secondary coil which receives the AC current and the bridge rectifier which converts the AC current into Dc current to be compatible with smartphones application because this device is charged only by DC.

In the transmitter side the type of inverter that used is half bridge which contains two switches. The type of switches are MOSFET which are more suitable for low current and voltage. In this study the voltage and current need is not high.

In the receiver side, the rectifier of bridge type with four diodes and Dc link capacitor at load is used to convert the AC signals (voltage, current) into DC signals and the capacitor's function is to smooth the voltage at output.

The target of this design is to get a 5V, 2A which leads to 10 W needed to charge some smart phones. So this result can be obtained depending on system parameter design that have been used, the frequency and the physical parameters such as distance coils specifications. So, all these parameter taken into account when designing the coils and all system. The system sections had been explained briefly in the next figures to know the utility of every part. Figure 3.6 shows the input stage of the system where the input voltage is DC and the capacitors instead of two DC source voltage at input.

3.4 Simulation Results of the Frequency Variation Effect.

The frequency has a high effect on the WPT system design. In this section, a WPT circuit had been designed and simulated by Matlab program. The parameters that had been used are shown in Table 3..

Table 3.5 Parameters of the WPT circuit of frequency variation simulation.

Parameter	Value
Inductance (L1)	25 μ H
Inductance (L2)	21 μ H
Resonance Frequency (Fr)	70 to 100 KHz
Distance	30 mm

The circuit is designed as shown in Fig 3.14 where different frequencies are used to the system to compare between the results and to shows the effect of the frequency variation on the system performance to achieve 5V and 2A.

Figure 3.12 shows the primary AC voltage and the current of the system after entering the inverter (inverter used to convert the DC to AC signal).

This figure also shows that the current and voltage are approximately 1.5A, and 12.88 Vpick whereas these values changes on the secondary side as shown in figure 4.10

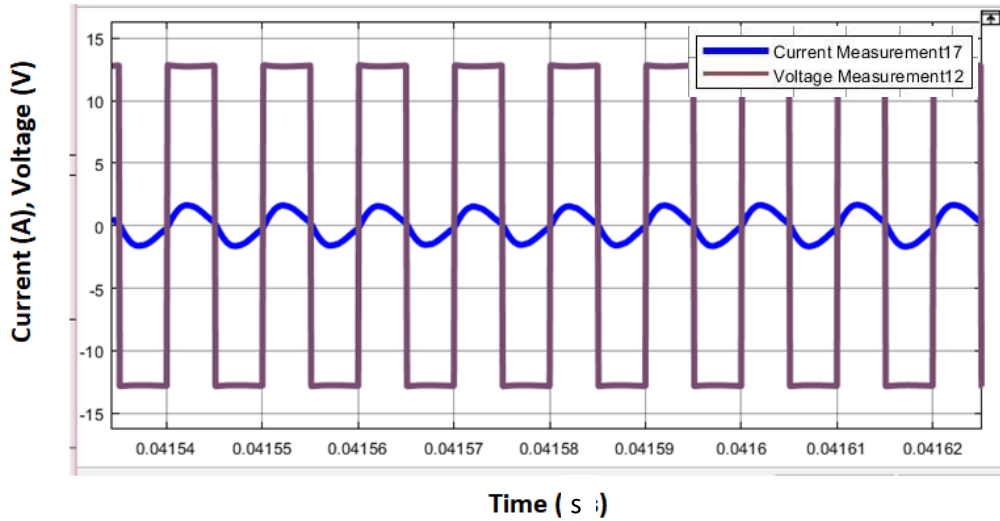


Figure. 3.14 Output of inverter I, V at Fr= 100 KHz.

Figure 3.13 shows the change in voltage and current values which are become 6V, 2.5A, that means the voltage is reduced and the current is increased. These signals will then enter into the rectifier to be converted into DC signals.

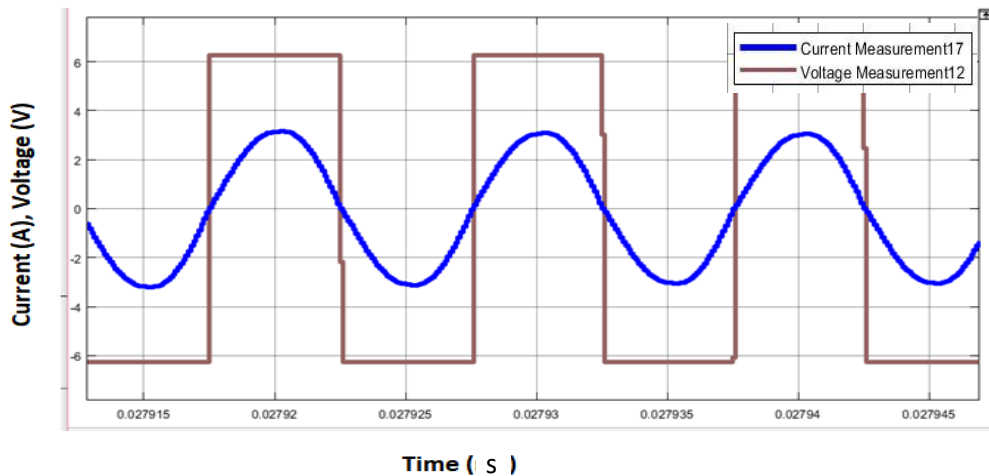


Figure 3.15 Current and voltage of the secondary coil at Fr= 100 KHz.

Figures 3.16 and 3.17 summarizes the change in current and voltage at the primary side at Fr =70 to 100 KHz.

Moreover, figure 3.16 clarify the changes in current at the input stage where the current is decreasing with the increasing of input resonance frequency.

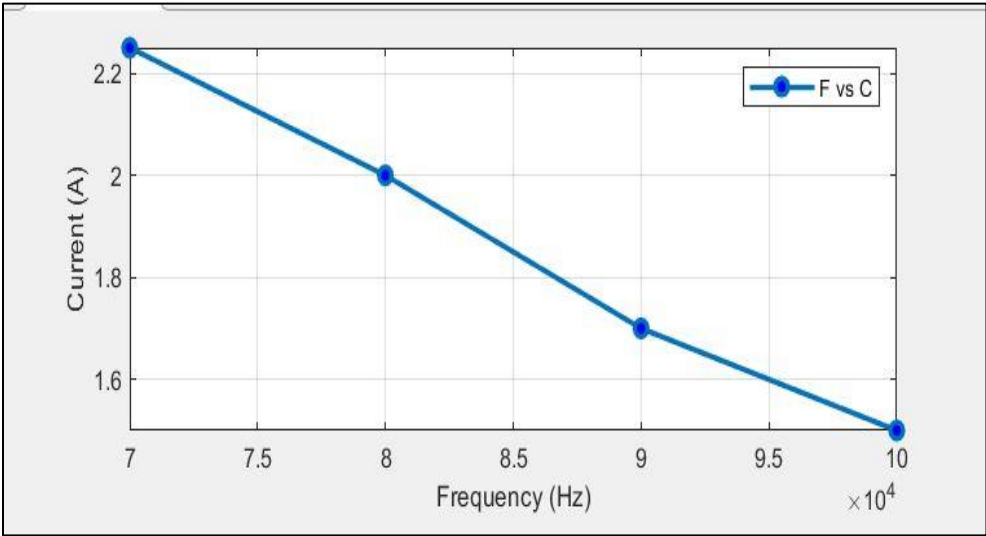


Figure 3.16 The current changing of the input stage at Fr from 70 to 100 KHz.

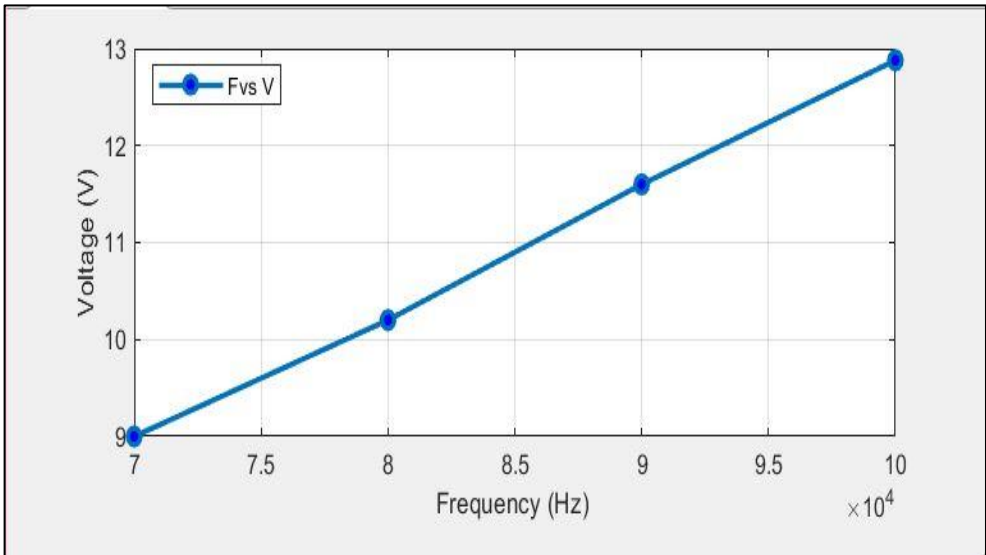


Figure 3.17 The voltage changing of the input stage at Fr from 70 to 100 KHz .

The voltage is increased in the input stage with the increase in frequency due to the relation between current and voltage which is, when the current decrease leads to needs voltage increasing as shown in figures 3.16, 3.17 to still get the required results in output .

3.5 Simulation Results of the Distance Variation Effect.

As discussed, many parameters can affect the system's performance. Distance also has an influence. In this section, the effect of distance variation on the system performance was simulated by MAT LAB program and the results show the effect of distance variation on the system such as on coupling coefficient and mutual inductance which will effect the system efficiency.

Coupling coefficient and mutual inductance have a major effect on the system where the weak coupling between two coils leads to a decrease the power transmission. So, the distance is an important parameter that should be considered when designing a system.

The system parameters shown in Table 3.6 are designed and chosen depend on on the dimension of the familiar smartphone specification to be compatible with them.

Table 3.6 Parameters of the smartphone charger proposed design.

Parameter	Value
TX coil length	200mm
RX coil length	185mm
Coils width	60mm
Coil inductance L1	33 μ H
Coil inductance L2	23 μ H
Resonance frequency	50 to 100 KHz
Number of turns (N1)	12
Number of turns (N2)	12
The gap between coils	30 mm

Figures 3.18 and 3.19 show the effect of distance variation on the coupling coefficient and mutual inductance.

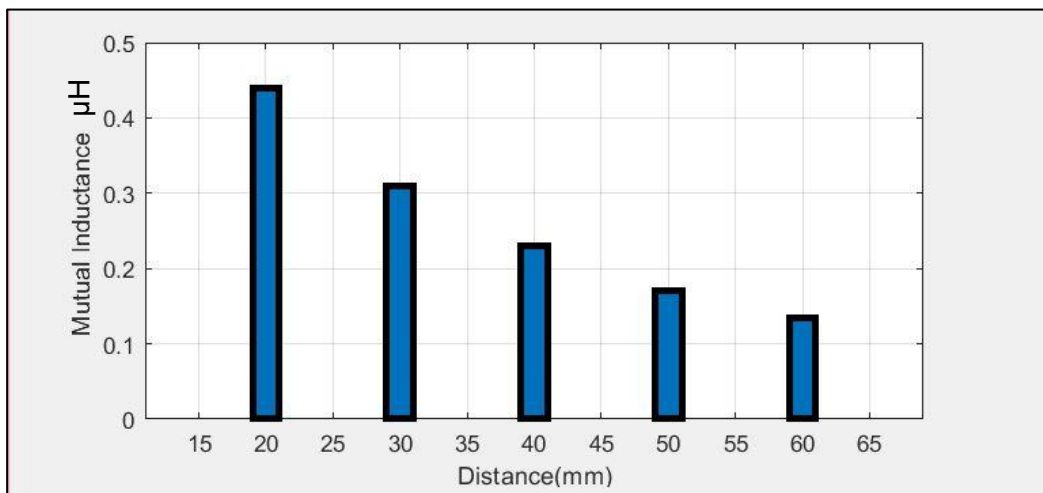


Figure 3.18 Mutual inductance at distance from 20 to 60mm

It can be noticed from figure 3.18 the mutual inductance is highly effective at the distance from 20 to 60 mm when the distance between two coils of the WPT system is increased leading to a decrease in the mutual inductance between coils.

Figure 3.19 explains the effect of the coupling coefficient when the distance is changed between 20 to 60 mm and this figure shows that the coupling coefficient is increased when the distance is decreased which means that there is a nonlinear relation between K and distance.

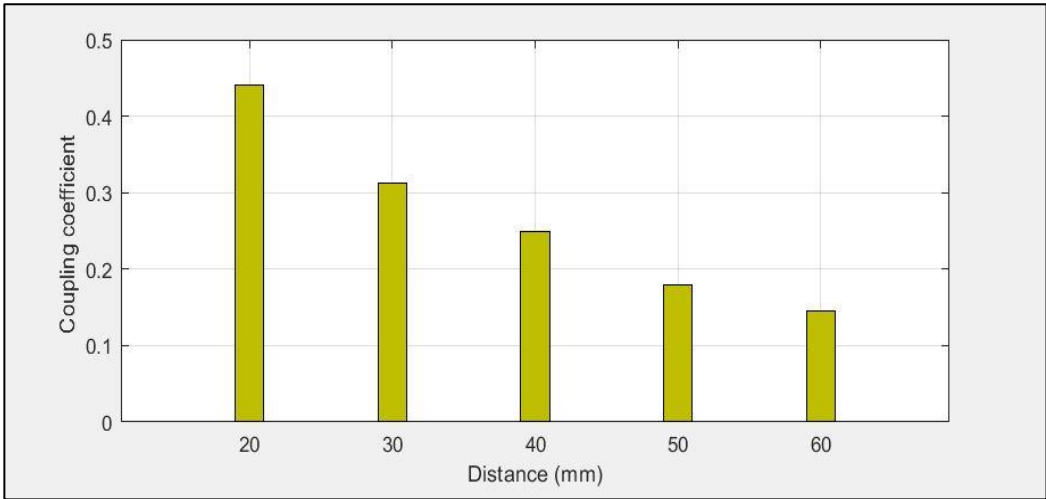


Figure 3.19 Coupling coefficient at distance from 20 to 60mm.

The summary of figures 3.18 and 3.19 explains the effect of distance variation on the system performance, where coupling coefficient and mutual inductance can highly affect efficiency and power transmission. The increase in distance leads to reducing the mutual inductance and coupling coefficient (K) where K is a portion of magnetic flux generated by the current in primary coil linked to the secondary coil, where increasing the distance mean the magnetic field is reduced and then the power transmitted efficiency (PTE) is reduced.

3.6 Simulation Results of WPT for Smartphone charging System

The parameters that used are the same as in Table 3.6, where in this section the frequencies that used are from 50 to 100 KHz to choose the best resonance frequency (F_r) of higher power transmitter efficiency.

Where the required results in this thesis are to charge a smartphone battery at 10 W with 5V and 2A.

3.6.1 Simulation Results of WPT for Smartphone charging System at $F_r = 50$ KHz

Figures 3.20 - 3.22 are the signals of voltage and current. These results are shown to compare the values with the other frequencies in the next section to choose the acceptable frequency and other parameters of the design to obtain the required results.

Figure 3.20 shows the MOSFET current at the primary stage the which is equal to 3A. This current then enter to the inverter to convert it to an Ac signal.

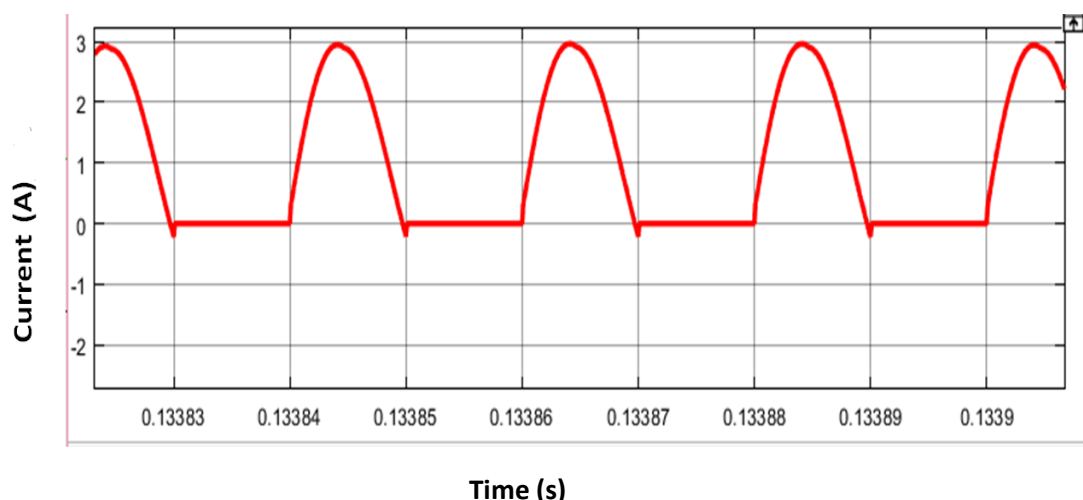


Figure 3.20 MOSFET current at $F_r = 50$ KHz.

Figure 3.21 shows the Ac current and voltage at the input stage which are the output of inverter at $f_r = 50 \text{ KHz}$

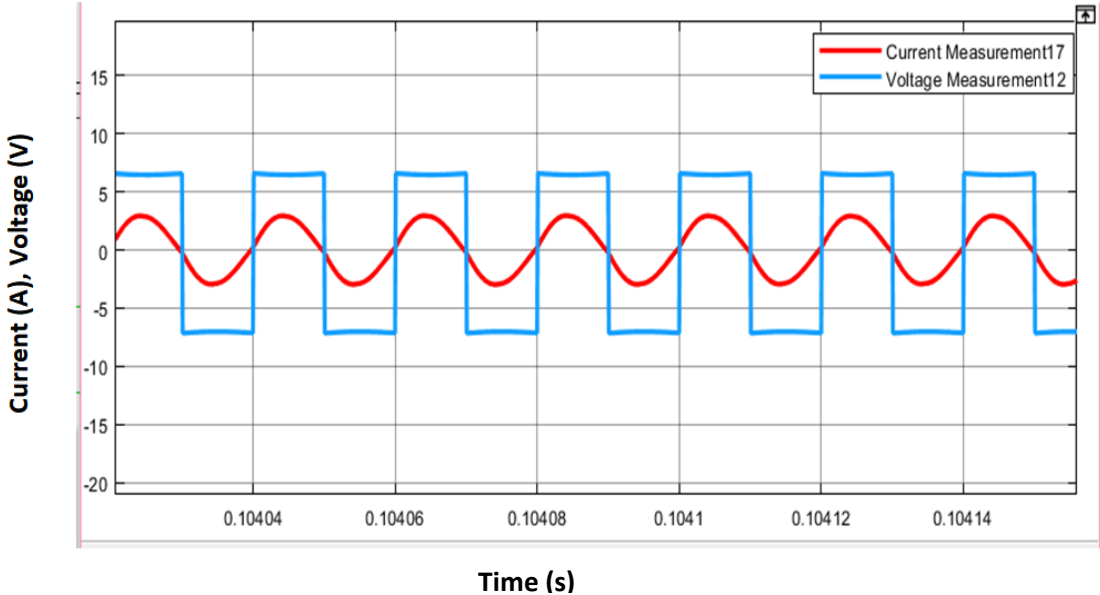


Figure 3.21 Signals of current and voltage at the primary stage of WPT system at $f_r = 50 \text{ KHz}$.

Figure 3.22 shows the AC signal of the current and voltage after being transmitted to the secondary coil where there is a small change in values due to the losses at the transmitting operation.

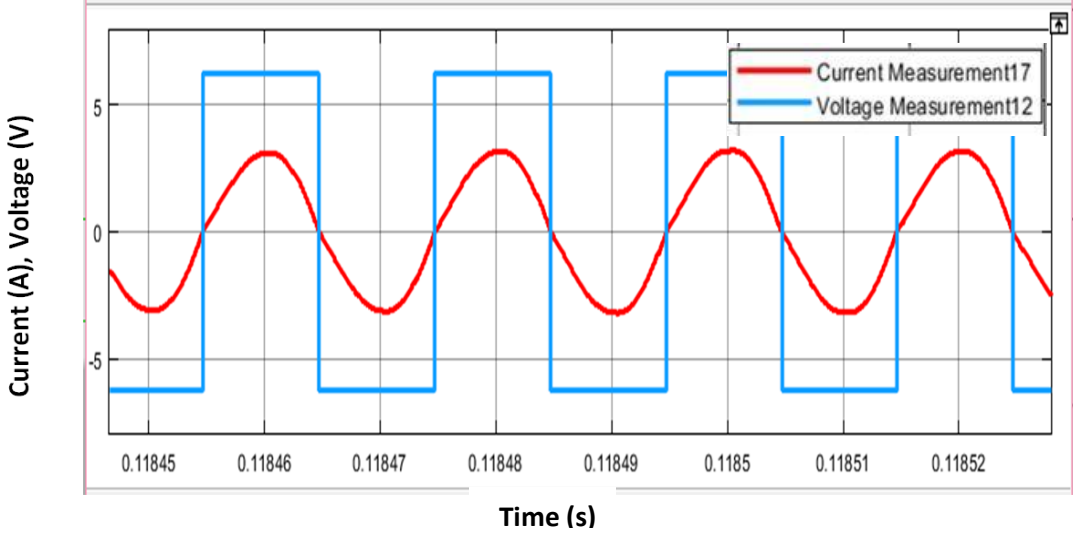


Figure 3.22 Signals of current and voltage at the secondary stage of WPT system at $f_r = 50 \text{ KHz}$.

3.6.2 Simulation Results of WPT for Smartphone charging System at $f_r = 60$ KHz.

In this section, the current of the input stage is shown and the current and voltage of the primary and secondary stage of the circuit at resonance frequency which is equal to 60 KHz are shown in figures 3.23, 3.24 and 3.25.

Figure 3.23 can show that the MOSFET current has been decreased to 2.5 A due to the increase in frequency.

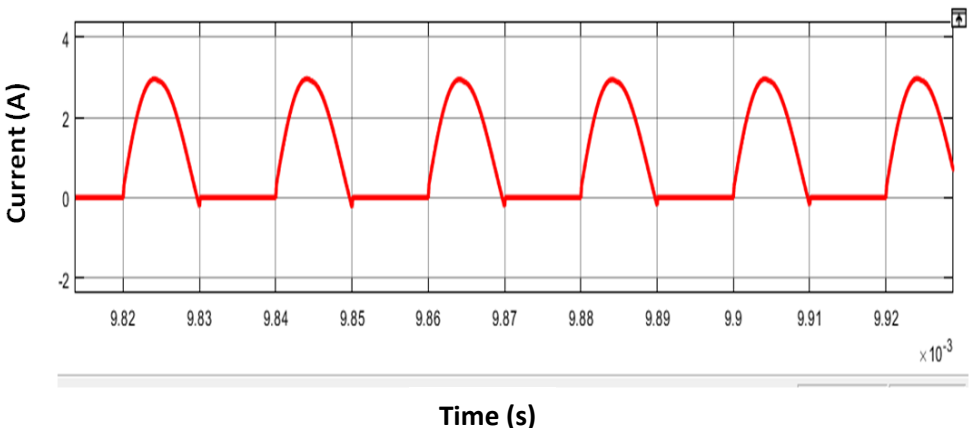


Figure 3.23 MOSFET current at $f_r = 60$ KHz.

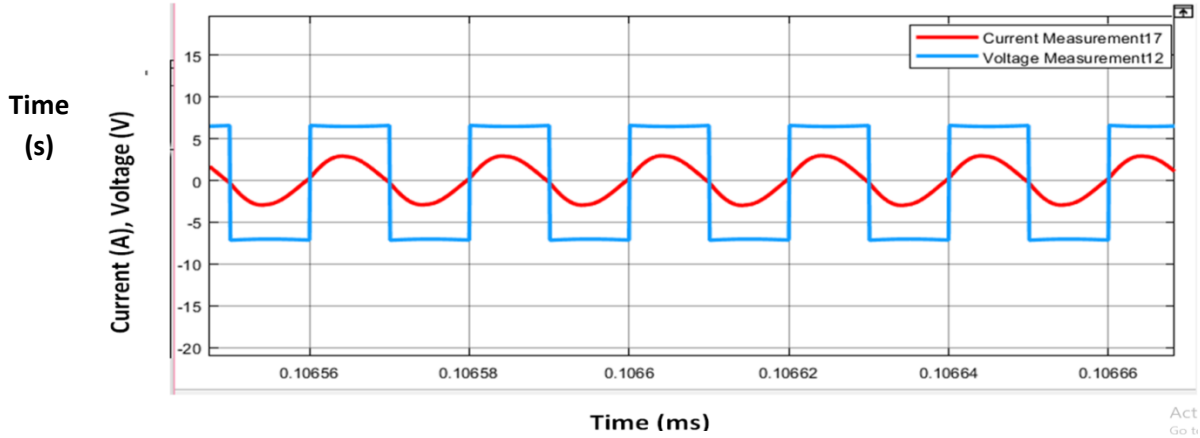


Figure 3.22 Signals of current and voltage at the primary stage of WPT system at $f_r = 60$ KHz.

The current and voltage after entering into the inverter are converted into Ac signals where the signals in figure 3.22 and the changing in values as the frequency increase can be noted.

Figure 3.23 shows the voltage and current at the receiver stage which are the Ac signals before entering the rectifier to be changed over to Dc signals.

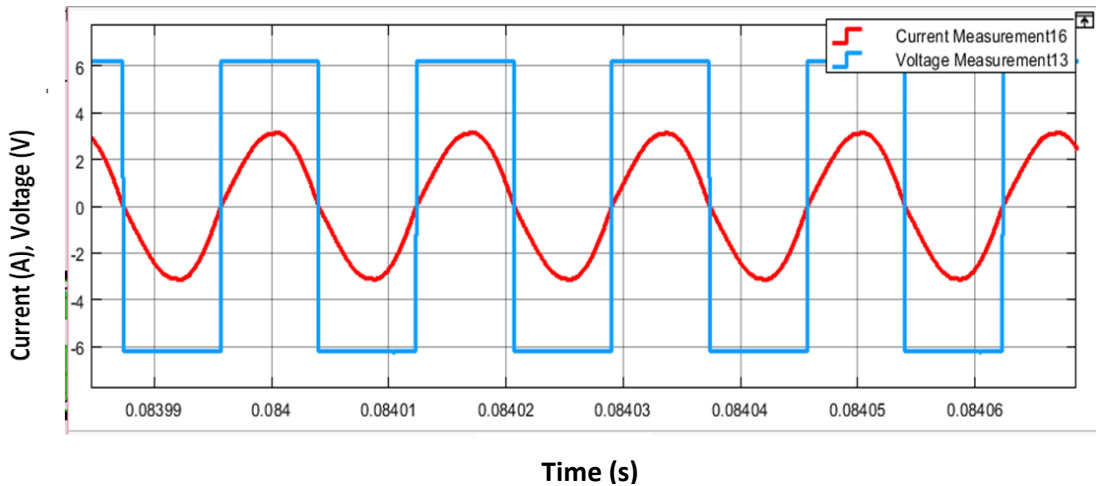


Figure 3.23 Signals of current and voltage at the secondary stage of WPT system at $f_r = 60$ KHz.

3.6.3 Simulation Results of WPT for Smartphone charging System at $f_r = 70$ KHz.

At $f_r = 70$ KHz can be noticed from figure 3.26 that the MOSFET (input) current becomes $I_{pick} = 2.12$ A whereas at $f_r = 60$ KHz the $I_{pick} = 2.5$ which is still decreasing in its value due to the frequency changing .

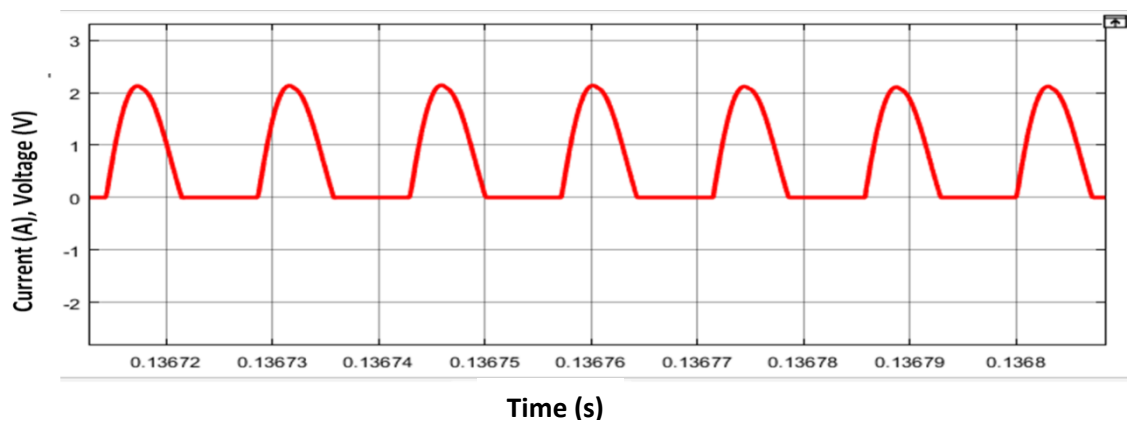


Figure 3.26 MOSFET current at $f_r = 70$ KHz.

It can be noticed from figure 3.27 that the AC current and voltage at the $f_r=70$ KHz and the changes in values from the primary stage to the secondary stage take place as shown in figure 3.28, where this changes in values are due to the losses when transmitting from one coil to another

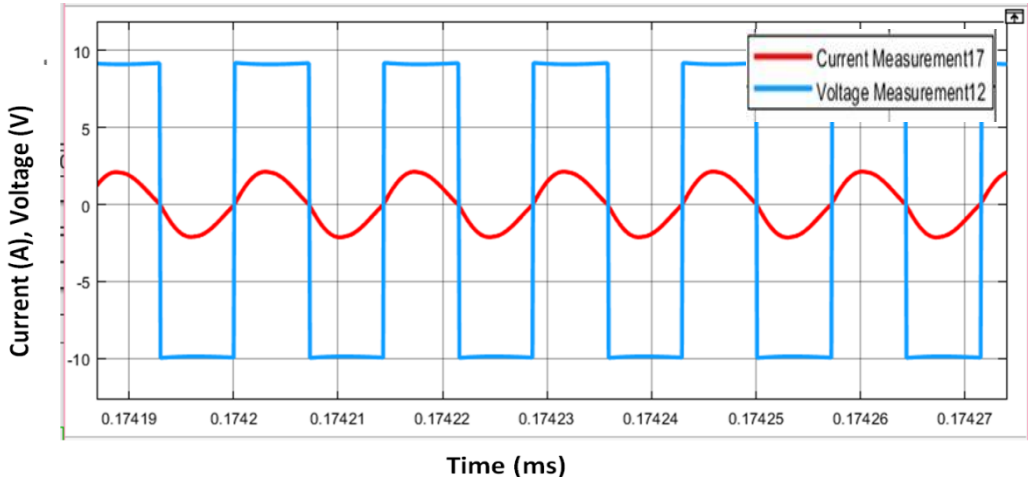


Figure 3.27 Signals of current and voltage at the primary stage of WPT system at $f_r=70$ KHz.

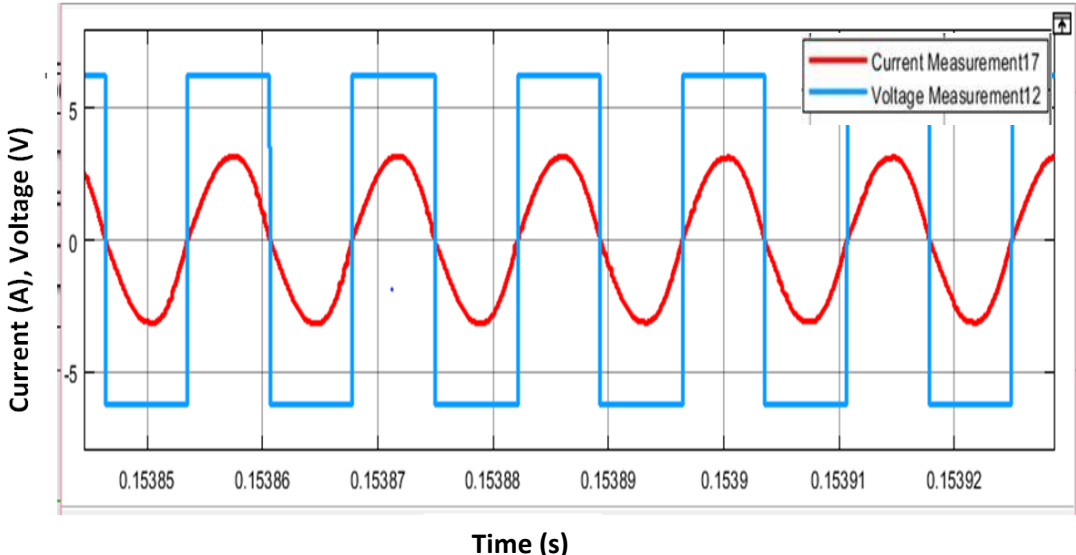


Figure 3.28 Signals of current and voltage at the secondary stage of WPT system at $f_r=70$ KHz.

3.6.4 Simulation Results of WPT for Smartphone charging System at $f_r = 80$ KHz.

At a resonance frequency equal to 80 KHz, the MOSFET current signal is shown in figure 3.29, and the current and voltage of the transmitter and receiving stage are shown in figures 3.30 and 3.31.

Figure 4.24 shows the input current is equal to 1.87A from this value that the current is decreased as the frequency increased can be seen which is considered a nonlinear relationship.

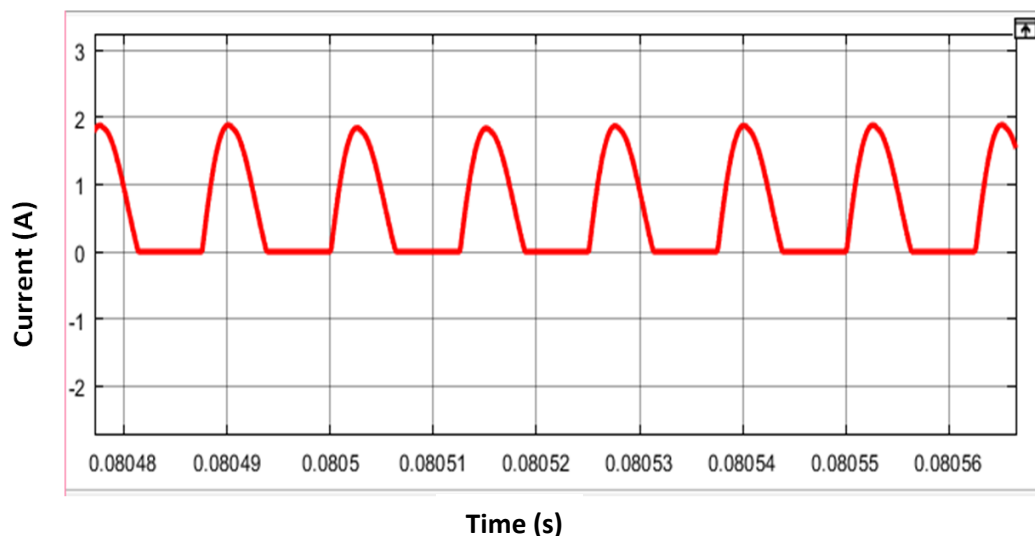


Figure 3.29 MOSFET current at $f_r = 80$ KHz.

Figures 3.30 and 3.31 show the AC current and voltage of the system at TX side and Rx side, where the voltage is decreased in the secondary side and the current increased. This change in values is for obtaining the required results.

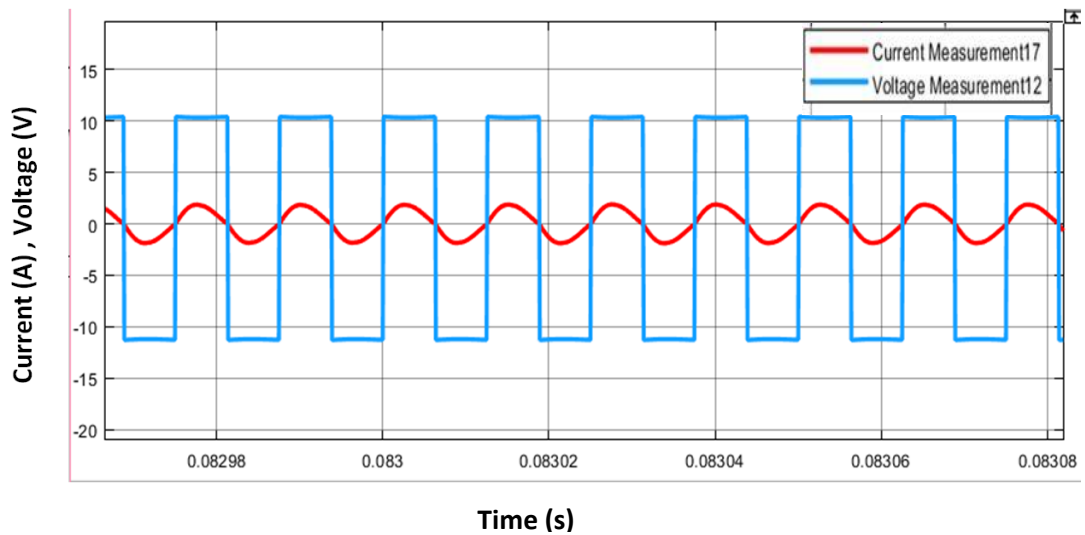


Figure 3.30 Signals of current and voltage at the primary stage of WPT system at $F_r= 80$ KHz.

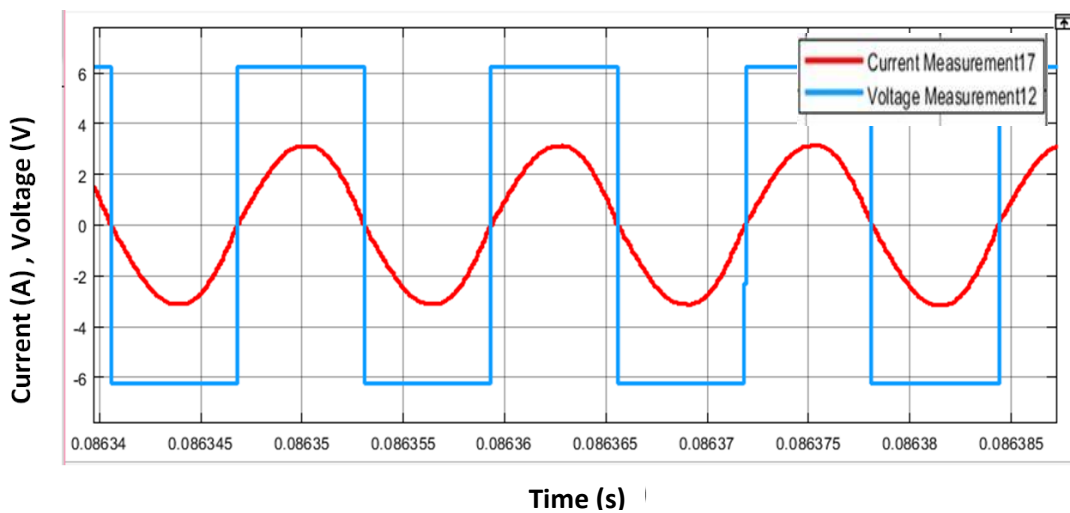


Figure 3.31 Signals of current and voltage at the secondary stage of WPT system at $F_r=80$ KHz.

3.6.5 Simulation Results of WPT for Smartphone charging System at $F_r =100$ KHz

In this section at resonance frequency equal to 100 KHz the required results with an acceptable efficiency compared to other sections are obtained.

It can be noticed that the current is decreased in value from 3 A at 50 KHz to 1.45A at 100 KHz as shown in figure 3.32. This decrease in current leads to an increase in the input voltage to compensate for the decreasing in input current as shown in Table 3.7.

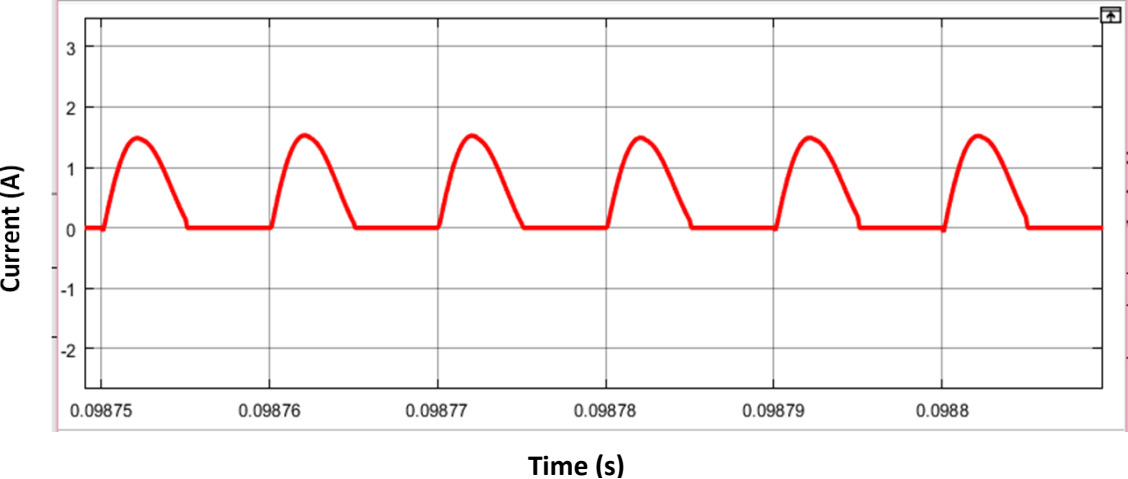


Figure 3. 32 MOSFET current at Fr=100 KHz.

It can be noticed from figures 3.33 and 3.34 that the changes in the current and voltage values where these changes are due to the frequency and input voltage changing

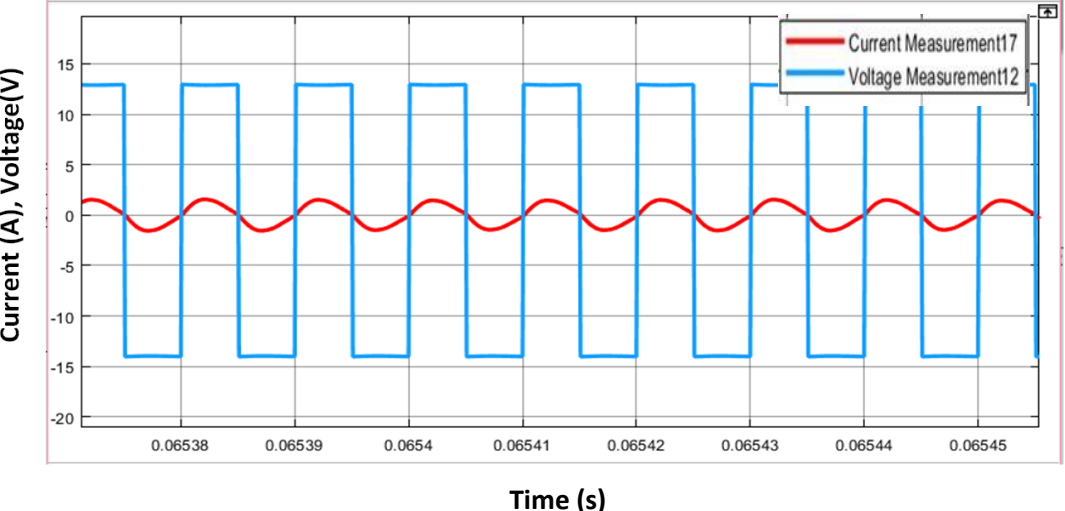


Figure 3. 33 Signals of current and voltage at the primary stage of WPT system at Fr= 100 KHz.

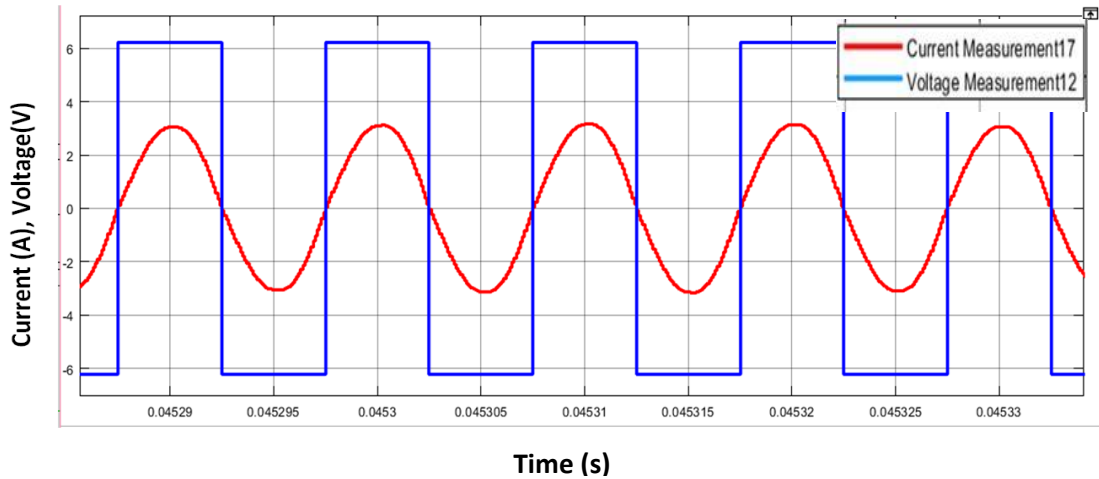


Figure 3.34 Signals of current and voltage at the secondary stage of WPT system at $f_r= 100$ KHz.

3.7 Results for Charging Smartphone Battery at $f_r=100$ KHz..

The required results for this study is to obtain a 10W with 5V, 2A at the output for each frequency with acceptable efficiency and the results obtained are shown in the figures 3.36 and 3.37. The output current (load current) is DC signal equal to 2A and the output voltage(load voltage) is DC signal equal to 5V then the result is to get power equal to 10W.

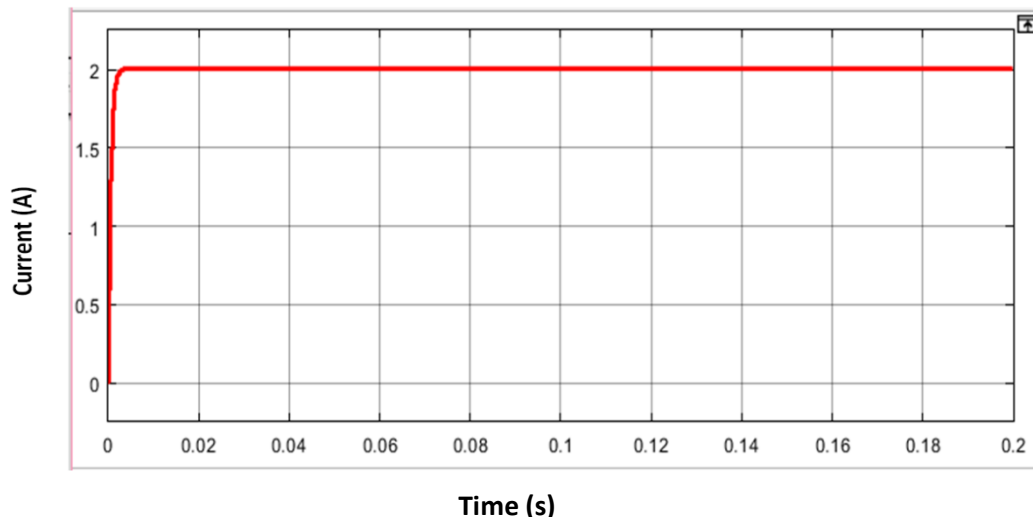


Figure 3. 36 Output Dc Current at $f_r=100$ KHz.

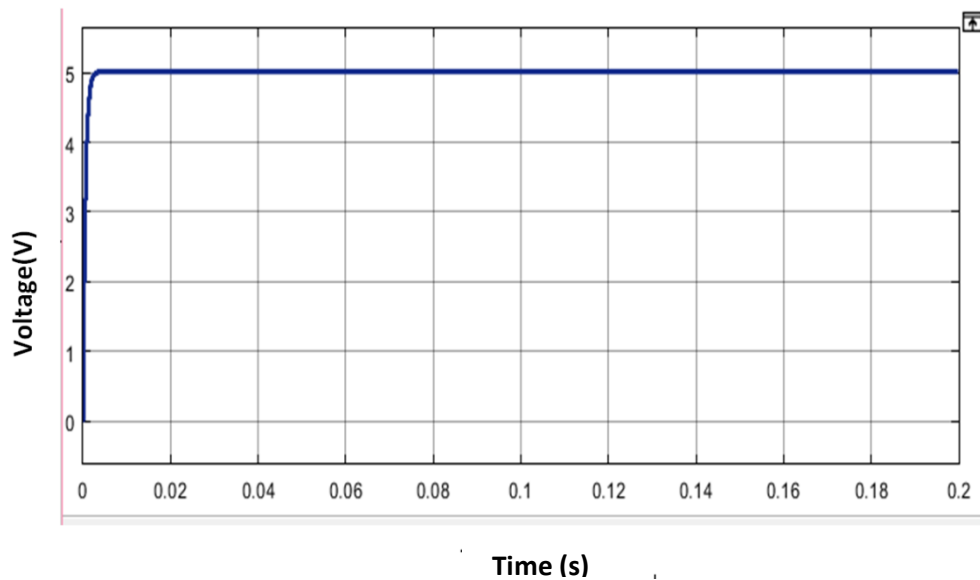


Figure 3. 37 Output Dc voltage at Fr=100 KHz.

The results in figures 3.36, 3.37 which are the voltage and current and the better results had been reached are at 100 KHz, because the efficiency for transmitting power is better and acceptable compared to the other frequencies, and the required system design is to get 10W for charging smartphone battery at better efficiency as shown in figure 3. 39.

Table 3.7 shows the results of the input and output current, input and output voltage and the input and output power at various frequencies. The resonance frequency is from 50 to 100 KHz and the change in power transmission at each resonance frequency can be noticed.

In the end, the results that had been reached is that the better power transmission is at 100 KHz compared to other frequencies values from 50-80 KHz. The efficiency variation of the system is shown and discussed in figure 3.33.

3.8 Results Discussion

Table 3.7 shows the obtained results of proposed charging system and it can be noticed that changing in resonance frequency effect on the input and current sources then the input power also effected. To obtain the required results a comparison among 5 frequencies values was used to choose the better system performance at the specific frequency. The summarize from table 3.7 that the better system performance and efficiency can obtained is at frequency equal to 100 KHz.

Table 3.7 Results of the smartphone charging proposed design.

Frequency (KHz)	I _{in} (rms) (A)	V _{in} (V)	I _{out} (A)	V _{out} (V)	P _{in} (W)	P _{out} (W)
50	2.12	6.6	2	5	13.99	10
60	1.76	7.83	2	5	13.81	10
70	1.49	9.2	2	5	13.708	10
80	1.3	10.4	2	5	13.52	10
100	1.02	12.9	2	5	13.185	10

It can be noticed from figure 3.38 the decrease in input current value from 2.12A at 50 KHz to 1.02A at 100 KHz as the frequency increases where this leads to needing to increase the input voltage to compensate for the decreasing in current as shown in figure 4.33. The voltage is increased from 6.6V at 50 KHz to 12.9V at 100 KHz.

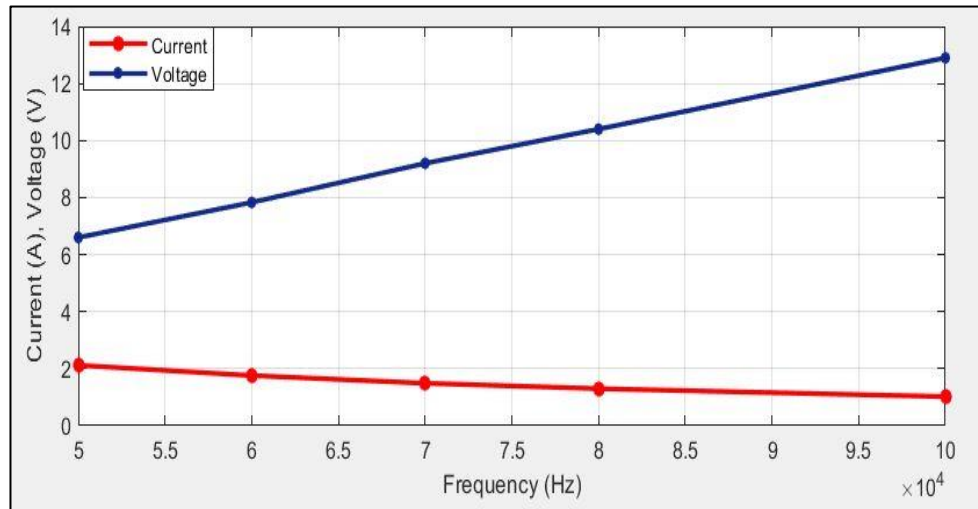


Figure 3.38 Input applied current and voltage at resonance frequency changing .

Figure 3.39 clarifies the efficiency at each resonance frequency from 50 to 100 KHz and the effect of frequency variation on the power transmitter efficiency (PTE) can be noticed. Table 3.7 and figure 3.39 shows that at resonance frequency of 100 KHz it is the better choice for designing the WPT system for charging smartphones applications where the efficiency is equal to 76 %.

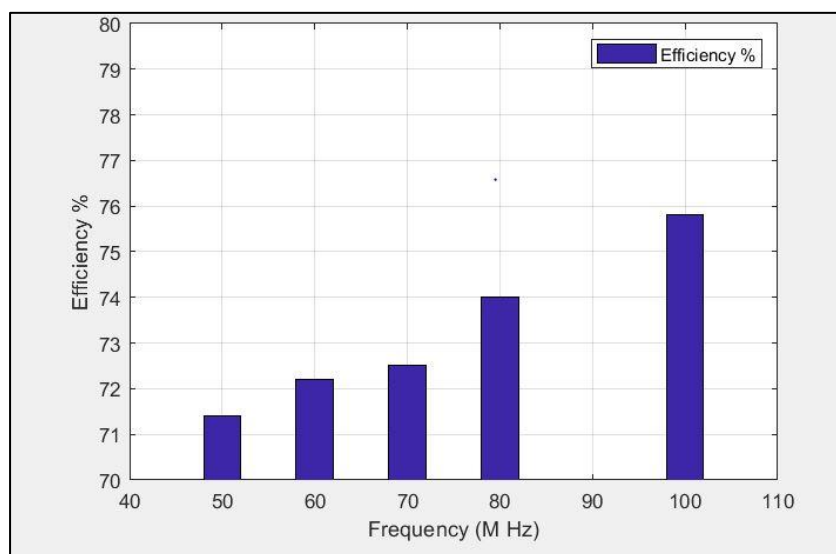


Figure 3. 39 Efficiency at resonance frequency from 50 to 100 KHz.

Figure 3.40 shows the effect of distance on the efficiency, when the distance increase the magnetic flux between two coils decrease which lead to decrease the mutual coupling between two coils then the power transmitted from the primary to the secondary coil is decrease and PTE is decrease.

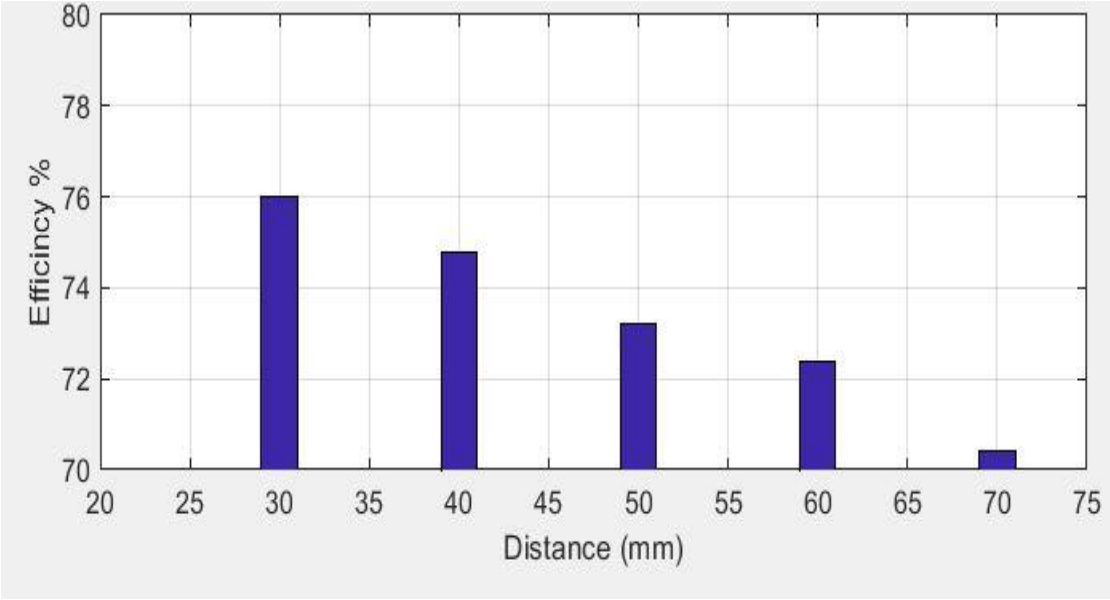


Figure 3. 40 Efficiency at different distances.

CHAPTER FOUR

Conclusions and Future Works

5.1 Conclusions

Resonance inductive coupling WPT system has been designed and simulated for charging smartphone applications.

There are many parameters that have an influence on the system efficiency. they are, the distance between coils, coupling factor, turn ratio, and resonance frequency. The switch inverter used is MOSFET because its suitable for low current and voltage. An appropriate resonance frequency and distance had been chosen to achieve the appropriate power transmitter efficiency which are 100KHz at 30mm . The design and simulation of the smartphone charger had been accomplished by MATLAB program.

The following are the points that had been reached and summarized in this thesis.

- If the distance between coils decreases, the coupling factor increases and the mutual inductance between coils is also increased. When the mutual between coils is high, the transmitted power between circuits becomes higher.
- Power transmitter efficiency can be improved when choosing the appropriate component values, resonance frequency and the physical, because the efficiency of the system depends on the closeness of the coils and the resonance frequency used in the circuit.
- MOSFET switch was used because it is suitable for low voltage operation.
- The performance of the Circuit design depends on the parameter that has been used such as inductance, turn ratio, compensation

circuit, resonance frequency, and the physical building which is the distance between coils.

- To charge the battery of smartphones, it need to consider the inputs and outputs power, voltage, and current variation because it needs a fixed output power.
- The increase in resonance frequency needs to increase in voltage source due to the current value decreasing to still get 10 W in the output.
- FSP occurred when the coupling factor is not at a critical value and exceeds this value .

5.2 Future Works

There are many ideas for WPT technology due to the features that can be attractive for numerous applications and users from the ease of use to the elimination complexity. So, it is important to develop this technique to obtain the benefits from it.

The following are future works that can added to enhance to envelop this study.

- ❖ This study can be practically implemented, but with some different parameter values if it is not available in markets.
- ❖ The efficiency can be increased by using 4 coils stages when designing the system.
- ❖ To charging more than device at the same time, more coils can added on the transmitter device.

- ❖ Adding a controller circuit to control the output voltage and current to be use this design with other applications that needs higher or lower voltages and also to be safe for all devices.

REFERENCE

- [1] T.Imura,"Wireless power transfer using magnetic electric resonance coupling techniques" Springer nature Singapore pte ltd, pp. 1-160, 2020.
- [2] I. Mayordomo, T. Dräger, P. Spies, J. Bernhard and A. Pflaum, "An Overview of Technical Challenges and Advances of Inductive Wireless Power Transmission," in Proceedings of the IEEE, vol. 101, no. 6, pp. 1302-1311, June 2013, doi: 10.1109/JPROC.2013.2243691.
- [3] R. E. Nafiaa and A. Z. Yonis," Investigation of High-Efficiency for Smartphone Applications"IEEE International Conference on Artificial Intelligence of Things(ICAIOT), Istanbul, Turkey, 2022.
- [4] L. Wang, T.Zhao, S.E.Chen, and D. Cook, "An Inductive Power Transfer System Design for Rail Applications". IEEE Transportation Electrification Conference and Expo (ITEC) pp. 84-89, June, 2018.
- [5] A.Mirta, "Simulation of Wireless Power Transfer", International Journal of Science Technology & Engineering, vol. 7, no.1, 2020.
- [6] J. Garnica, R. A. Chinga and J. Lin, "Wireless Power Transmission: From Far Field to Near Field," in Proceedings of the IEEE, vol. 101, no. 6, pp. 1321-1331, June 2013, doi: 10.1109/JPROC.2013.2251411.
- [7] S. Luo, S. Li and H. Zhao, "Reactive power comparison of four-coil, LCC and CLC compensation network for wireless power transfer" IEEE PELS Workshop on Emerging Technologies: Wireless Power Transfer (WoW), Chongqing, China, pp. 268-271, 2017, doi: 10.1109/WoW.2017.7959407.
- [8] K. Hata, T. Imura and Y. Hori, "Maximum efficiency control of wireless power transfer via magnetic resonant coupling considering dynamics of DC-DC converter for moving electric vehicles," IEEE

- Applied Power Electronics Conference and Exposition (APEC), Charlotte, NC, USA, 2015, pp. 3301-3306, doi: 10.1109/APEC.2015.7104826.
- [9] R. E. Nafiaa and A. Z. Yonis, "Performance Analysis of High-Efficiency WPT for Communication Technologies," 2022 14th International Conference on Computational Intelligence and Communication Networks (CICN), Al-Khobar, Saudi Arabia, 2022, pp. 78-82, doi: 10.1109/CICN56167.2022.10008337.
- [10] B. S. P. S. Manohar, V. V. S. K. Gandham, and P. K. Dhal. "An Overview of Wireless Power Transmission System and Analysis of Different Methods." *International Journal for Research in Applied Science and Engineering Technology* 3 (2022).
- [11] M. S. Mastoi, S. Zhuang, H. M. Munir, M. Haris, M. Hassan, M. Alqarni, B. Alamri, "A study of charging-dispatch strategies and vehicle-to-grid technologies for electric vehicles in distribution networks", *Energy Reports*, vol.9, pp. 1777-1806, 2023, <https://doi.org/10.1016/j.egyr.2022.12.139>.
- [12] K. Aditya and S. S. Williamson, "Comparative study of series-series and series-parallel topology for long track EV charging application," 2014 IEEE Transportation Electrification Conference and Expo (ITEC), Dearborn, MI, USA, 2014, pp. 1-5, doi: 10.1109/ITEC.2014.6861793.
- [13] A.T. Satel. "Wireless Charger for Low Power Devices", Master's thesis in Electrical and Computer Engineering Specialization in Telecommunications, Portugal, 2016.
- [14] Z. Liu, Z. Chen and J. Li, "A Magnetic Tank System for Wireless Power Transfer," in *IEEE Microwave and Wireless Components Letters*, vol. 27, no. 5, pp. 443-445, May 2017, doi: 10.1109/LMWC.2017.2690881.

- [15] Z. Zhang, H. Pang, A. Georgiadis, and C. Cecati, "Wireless Power Transfer—An Overview," in *IEEE Transactions on Industrial Electronics*, vol. 66, no. 2, pp. 1044-1058, Feb. 2019, doi: 10.1109/TIE.2018.2835378.
- [16] S. Kuka, Ni, Kai and M. Alkahtani. "A Review of Methods and Challenges for Improvement in Efficiency and Distance for Wireless Power Transfer Applications" *Power Electronics and Drives*, vol.5, no.1, 2020, pp.1-25
- [17] M. Amjad, M. F.I.Azam, Q.Ni, M. Dong, E.H. Ansari, "Wireless charging systems for electric vehicles." *Renewable and Sustainable Energy Reviews* vol. 1670, pp.112730, 2022.
- [18] Y. Zhang, S. Chen, X. Li and Y. Tang, "Design of high-power static wireless power transfer via magnetic induction: An overview," in *CPSS Transactions on Power Electronics and Applications*, Vol. 6, No.4, pp. 281-297, Dec, 2021, doi: 10.24295/CPSSTPEA.2021.00027.
- [19] W. Zhang, D. Xu, and R. Hui, "Wireless power transfer between distance and efficiency", Springer Nature Singapore, pp. 1-16, 2020.
- [20] N. Robabeh, "Development of a Resonant High Power Charging Station for Fleet Vehicles". *Theses and Dissertations*, 2105, 2019, <https://dc.uwm.edu/etd/2105>.
- [21] C.Rong, C.Lu, Y.Zeng, X.Tao, X.Liu, R.Liu, X.He and M.Liu, "A critical review of metamaterial in wireless power transfer system, *IET Power Electronics*"pp. 1541-1559, 2021.
- [22] J. Tritschler, B.Goeldi, S. Reichert, and G. Griepentrog, "Comparison of different control strategies for series-series compensated inductive power transmission systems". In *IEEE 17th European Conference on Power Electronics and Applications (EPE'15 ECCE-Europe)* pp. 1-8, 2015, doi: 10.1109/EPE.2015.7309309.

- [23] J. Liu, Z. Wang and M. Cheng, "Optimization of Coils for Wireless Power Transfer System in Electric Vehicle," 2018 21st International Conference on Electrical Machines and Systems (ICEMS), Jeju, Korea (South), 2018, pp. 2161-2165, doi: 10.23919/ICEMS.2018.8549011.
- [24] J. Y. Hou, Y.Cao, H.Zeng, T.Hei, X.G. Liu,and M.H.Tian, "High efficiency wireless charging system design for mobile robots". In IOP Conference Series: Earth and Environmental Science Vol. 188, No. 1, , Oct 2018.
- [25] H. A. Fadhil, S. G. Abdulqader and S. A. Aljunid, "Implementation of wireless power transfer system for Smart Home applications," 2015 IEEE 8th GCC Conference & Exhibition, Muscat, Oman, pp. 1-4, 2015 doi: 10.1109/IEEEGCC.2015.7060042.
- [26] D. Dai and J. Liu, "Human powered wireless charger for low-power mobile electronic devices," in IEEE Transactions on Consumer Electronics, vol. 58, no. 3, pp. 767-774, August 2012, doi: 10.1109/TCE.2012.6311316.
- [27] S. H. Yusoff, N. N. Nanda, N. S. Midi and A. S. Abed Badawi, "Mathematical Design of Coil Parameter for Wireless Power Transfer using NI Multisims Software," 2021 8th International Conference on Computer and Communication Engineering (ICCCE), Kuala Lumpur, Malaysia, pp. 99-103, 2021 doi: 10.1109/ICCCE50029.2021.9467166.
- [28] A. I. Mahmood, S. K. Gharghan, M. A. A. Eldosoky, M. F. Mahmood and A. M. Soliman, "Wireless Power Transfer Based on Spider Web–Coil for Biomedical Implants," in IEEE Access, vol. 9, pp. 167674-167686, 2021, doi: 10.1109/ACCESS.2021.3136817.
- [29] M. Abou Houran, X. Yang, W.Chen, "Magnetically Coupled Resonance WPT: Review of Compensation Topologies, Resonator Structures with Misalignment, and EMI Diagnostics". Electronics ,vol.7, no.11,2018, <https://doi.org/10.3390/electronics7110296>

- [30] A.T.Cabrera, J.G.Gonza, J.Aguado, " Wireless Power Transfer for Electric Vehicles: Foundations and Design Approach" Springer nature Switzerland AG, pp 1-140., 2020.
- [31] O.Singh, "Wireless Mobile Charger", International Journal of Electronics, Electrical and Computational System, Vol.5, No.6, June 2016.
- [32] M. S.Y.R. Hui, W.X. Zhong , and C.K. Lee, "A Critical Review of Recent Progress in Mid-Range Wireless Power Transfer" IEEE Trans. Ind. Electron., vol. 61, no. 7, pp. 1–4, 2013.
- [33] J.Van Mulders, D. Delabie, C.Lecluyse, C. Buyle, G. Callebaut, L.Van der Perre, and L. De Strycker, "Wireless Power Transfer: Systems, Circuits, Standards, and Use Cases". Sensors ,vol 22:5573. 2022, doi.org/10.3390/s22155573
- [34] B. Zhai, M. Yang and G. Liu, "Trim method of impedance matching for magnetic resonance coupling system" 29th Chinese Control And Decision Conference (CCDC), Chongqing, China , pp. 2157-2161, 2017, doi: 10.1109/CCDC.2017.7978872.
- [35] B. Minnaert and N. Stevens, "Maximizing the Power Transfer for a Mixed Inductive and Capacitive Wireless Power Transfer System" IEEE Wireless Power Transfer Conference (WPTC), Montreal, QC, Canada, 2018, pp. 1-4, doi: 10.1109/WPT.2018.8639265.
- [36] Y. Zhang, S. Chen, X. Li, Z. She, F. Zhang and Y. Tang, "Coil Comparison and Downscaling Principles of Inductive Wireless Power Transfer Systems," IEEE PELS Workshop on Emerging Technologies: Wireless Power Transfer (WoW), Seoul, Korea (South), pp. 116-122, 2022, doi: 10.1109/WoW47795.2020.9291295.
- [37] A.Ahmad, " Analysis of Wireless Charging Schemes for Electric Vehicles", Thesis, 2019

- [38] M. Dharani, and R. KB, "Systematic literature review on wireless power transmission", *Turk. J. Comput. Math. Educ*, vol 12, no 10 pp. 4400-4406, 2021.
- [39] C. Degen, "Inductive coupling for wireless power transfer and near-field communication", *EURASIP Journal on Wireless Communications and Networking*, vol.1, pp 1-20, Dec 2021.
- [40] S. I. Kamarudin, A. Ismail, A. Sali, and M .Y. Ahmad, "Magnetic resonance coupling for 5G WPT applications", *Bulletin of Electrical Engineering and Informatics* vol.8.no.3, pp.1036-1046, 2019.
- [41] P.Jeebklum, P. Kirawanich, and C. Sumpavakup, "Dynamic Wireless Power Transfer with a Resonant Frequency for Light Duty Electric Vehicle", vol.14, no.6, 2021, DOI: 10.22266/ijies2021.1231.37.
- [42] T. S. Pham, T. D. Nguyen, B.S. Tung, B. X. Khuyen, T. T. Hoang, Q. M. Ngo, L. H. Hiep and V. D. Lam," Optimal frequency for magnetic resonant wireless power transfer in conducting medium". *Scientific Report* vol.11, 2021, <https://doi.org/10.1038/s41598-021-98153-y>.
- [43] P. Joshi, "Measure the Efficiency of Energy Transfer Systems Under External Influences and Model How the Resonance Frequency is Influenced Under Such Conditions", M.Sc Thesis, University of Bergen, 2014.
- [44] M. Wang, L. Ren, Y. Shi, W. Liu, H. R. Wang, "Analysis of a nonlinear magnetic coupling wireless power transfer system." *Progress In Electromagnetics Research C* Vol.110, pp.15-26, 2021.
- [45] Y.Zhang, "Design of High Efficiency Wireless Power Transfer System with Nonlinear Resonator", Diss, University of South Carolina, 2020.
- [46] T. Thabet, and J. Woods, "A Solution to Frequency Splitting in Magnetic Resonance Wireless Power Transfer Systems Using Double

- Sided Symmetric Capacitors". European Journal of Electrical Engineering and Computer Science, Vol.5, No2, 6-12, 2021
- [47] R. K. Pokharel, A. Barakat, F. Tahar and S. Hekal, "Degree of Freedom to Select Coupling Coefficient and Quality Factor in Near-Field Wireless Power Transfer: A Case Study of Using DGS Structures" IEEE MTT-S International Microwave and RF Conference (IMaRC), Ahmedabad, India, pp. 1-5, 2017, doi: 10.1109/IMaRC.2017.8449719.
- [48] X. Li, X. Dai, Y. Li, Y. Sun, Z. Ye and Z. Wang, "Coupling coefficient identification for maximum power transfer in WPT system via impedance matching," IEEE PELS Workshop on Emerging Technologies: Wireless Power Transfer (WoW), pp. 27- 30, 2016.
- [49] S. Baroi, M. S. Islam and S. Baroi, "Design and Simulation of Different Wireless Power Transfer Circuits," 2017 2nd International Conference on Electrical & Electronic Engineering (ICEEE), Rajshahi, Bangladesh, pp. 1-4, 2017, doi: 10.1109/CEEE.2017.8412874.
- [50] A. Pusti, P. K. Das, A. K. Panda, J. Padhi and D. P. Kar, "Essential Analysis of MRC-WPT System for Electric Vehicle Charging Using Coupled Mode Theory" 1st Odisha International Conference on Electrical Power Engineering, Communication and Computing Technology(ODICON), Bhubaneswar, India, pp. 1-5, 2021, doi: 10.1109/ODICON50556.2021.9429020.
- [51] Y.Liu, S.Bai, W.Zhang and K. Li, "Design and optimization of mutual inductance for high efficiency ICPT system" IEEE 8th International Power Electronics and Motion Control Conference (IPEMC-ECCE Asia), Hefei, pp. 3178-3182, 2016, doi: 10.1109/IPEMC.2016.7512804.

- [52] Z. -J. Liao, Y. Sun, Z. -H. Ye, C. -S. Tang and P. -Y. Wang, "Resonant Analysis of Magnetic Coupling Wireless Power Transfer Systems," in *IEEE Transactions on Power Electronics*, Vol. 34, No. 6, pp. 5513-5523, June 2019, doi: 10.1109/TPEL.2018.2868727..
- [53] H. Matsumoto, N. Khan and O. Trescases, "A 5kW Bi-directional Wireless Charger for Electric Vehicles with Electromagnetic Coil based Self-Alignment," *IEEE Applied Power Electronics Conference and Exposition (APEC)*, Anaheim, CA, USA, , pp. 1508-1514, 2019, doi: 10.1109/APEC.2019.8722298.
- [54] C.Panchal, S.Stegen, and J.Lu, "Review of static and dynamic wireless electric vehicle charging system". *Engineering science and technology, an international journal*, vol. 21, no.5, pp. 922-937, 2018.
- [55] M. Galizzi, M. Caldara, V. Re and A. Vitali, "A novel Qi-standard compliant full-bridge wireless power charger for low power devices," *2013 IEEE Wireless Power Transfer (WPT)*, Perugia, Italy, pp. 44-47, 2013, doi: 10.1109/WPT.2013.6556877.
- [56] M. H. Rashid, N. Kumar, and A. R. Kulkarni," *Power electronics: devices, circuits and applications.*" Book, Pearson Education Limited, pp.307-3019, 2014.
- [57] M. H. Rashid, " *Power electronics handbook*", Book, Academic express, Florida , pp. ,139-144, 2001.
- [58] R. O. Caceres and I. Barbi, "A boost DC-AC converter: analysis, design, and experimentation," in *IEEE Transactions on Power Electronics*, vol. 14, no. 1, pp. 134-141, Jan. 1999, doi: 10.1109/63.737601.
- [59] M. -T. Kuo and S. -D. Lu, "A study of DC-AC inverter optimization for photovoltaic power generation system," *2012 IEEE Industry Applications Society Annual Meeting*, Las Vegas, NV, USA, 2012, pp.

- 1-7, doi: 10.1109/IAS.2012.6374000.C. W. Lander, "Power Electronics", Book, 3rd ed. The McGraw-Hill Companies London 1993.
- [60] A. Trzynadlowski, INTRODUCTION TO MODERN POWER ELECTRONICS, Book, 3rd ed, 2016.
- [61] K H. Sueker, "Power electronics design: a practitioner's guide", Book, Elsevier, 2005.
- [62] A. Pacini, A. Costanzo, S. Aldhafer and P. D. Mitcheson, "Design of a position-independent end-to-end inductive WPT link for industrial dynamic systems" IEEE MTT-S International Microwave Symposium (IMS), Honolulu, HI, USA, pp. 1053-1056, 2017, doi: 10.1109/MWSYM.2017.8058774.
- [63] J.L.Villa, A. Llombart, J.F.Sanz , and, J.Sallan "Development of an inductively coupled power transfer system (ICPT) for electric vehicles with a large airgap", Electric Engineering Department, University of Zaragoza C/María de Luna 3, 50018, Zaragoza, Spain, vol.1,no.5, 2007.
- [64] J. P. K. Sampath, A. Alphones, and H. Shimasaki, "Coil design guidelines for high efficiency of wireless power transfer (WPT)" IEEE Reg. 10 Annu. Int. Conf. Proceedings/TENCON, vol. 1, no. c, pp. 726–729, 2017.
- [65] L. Wang, T. Zhao, S. -E. Chen and D. Cook, "An Inductive Power Transfer System Design for Rail Applications," 2018 IEEE Transportation Electrification Conference and Expo (ITEC), Long Beach, CA, USA, pp. 84-89, 2018, doi: 10.1109/ITEC.2018.8450168.
- [66] R .E.Nafiaa, A .Z.Yonis, " Magnetic resonance coupling wireless power transfer for green technologies", Indonesian Journal of Electrical Engineering and Computer Science, vol. 26, no. 1, pp.289-295, April 2022".

- [67] M. ozman, M.Fernando, B. Adebisi, K.M.Rabie, R.Kharel, A.Ikpehai, and H.Gacanin, " Combined Conformal Strongly-Coupled Magnetic Resonance for Efficient Wireless Power Transfer", *Energies*, vol.10, no.498, 2017.
- [68] A. Abdolkhani, A. P. Hu, M. Moridnejad and A. Croft, "Wireless charging pad based on travelling magnetic field for portable consumer electronics," *IECON 2013 - 39th Annual Conference of the IEEE Industrial Electronics Society*, Vienna, Austria, 2013, pp. 1416-1421, doi: 10.1109/IECON.2013.6699340.
- [69] X. Liu, X. Yuan, C. Xia and X. Wu, "Analysis and Utilization of the Frequency Splitting Phenomenon in Wireless Power Transfer Systems," in *IEEE Transactions on Power Electronics*, vol. 36, no. 4, pp. 3840-3851, April 2021, doi: 10.1109/TPEL.2020.3025480
- [70] R. Huang, B. Zhang, D. Qiu and Y. Zhang, "Frequency Splitting Phenomena of Magnetic Resonant Coupling Wireless Power Transfer," in *IEEE Transactions on Magnetics*, vol. 50, no. 11, pp. 1-4, Nov. 2014, Art no. 8600204, doi: 10.1109/TMAG.2014.2331143.
- [71] A. Krivchenkov and R. Saltanovs. "Increasing the efficiency of the wireless charging system for mobile devices that support Qi standard." *Reliability and Statistics in Transportation and Communication: Selected Papers from the 18th International Conference on Reliability and Statistics in Transportation and Communication, RelStat'*, vol. no.18, pp.17-20 Oct 2018, Riga, Latvia 18. Springer International Publishing, 2019.
- [72] R. E. Nafiaa and A. Z. Yonis, "Analysis of Frequency Splitting Phenomenon in WPT for Intelligent Applications," 2022 *IEEE International Conference on Automatic Control and Intelligent Systems (I2CACIS)*, Shah Alam, Malaysia, 2022, pp. 174-179, doi: 10.1109/I2CACIS54679.2022.9815489.

RESESRCH PUBLICATION

The following are a list of publishing papers resulting of the work done in this thesis

- [1] R.E.Nafiaa, Aws.Z.Yonis, " Magnetic resonance coupling wireless power transfer for green technologies", Indonesian Journal of Electrical Engineering and Computer Science, vol. 26, no. 1, pp.289-295, April 2022"(Scopus).
- [2] R. E. Nafiaa and A. Z. Yonis, "Analysis of Frequency Splitting Phenomenon in WPT for Intelligent Applications" IEEE International Conference on Automatic Control and Intelligent Systems (I2CACIS), Shah Alam, Malaysia, 2022, pp. 174-179, doi: 10.1109/I2CACIS54679.2022.9815489. (Scopus).
- [3] R. E. Nafiaa and A. Z. Yonis, "Performance Analysis of High-Efficiency WPT for Communication Technologies" 14th International Conference on Computational Intelligence and Communication Networks (CICN), Al-Khobar, Saudi Arabia, 2022, pp. 78-82, doi: 10.1109/CICN56167.2022.10008337(Scopus).
- [4] R. E. Nafiaa and A. Z. Yonis," Investigation of High-Efficiency for Smartphone Applications" IEEE International Conference on Artificial Intelligence of Things(ICAIOT), Istanbul, Turkey, 2022.(Scopus).

الخلاصة

أصبحت تقنية نقل الطاقة اللاسلكية الآن من أهم التقنيات ومحط اهتمام العلماء. حيث أن مبدأ هذه التقنية هو إرسال الطاقة من جهاز مرسل الى اخر مستقبل دون اتصال فيزيائي بين الجهازين. إن نوع تقنية WPT التي تم استخدامها هو الاقتران الحثي ، نظرًا لسهولة عملها وأمنها مقارنة بتقنيات نقل الطاقة التقليدية.

الهدف من هذه الدراسة هو تصميم نظام لاسلكي ليكون قادرًا على نقل الطاقة أو شحن الهواتف الذكية بقدرة مقدارها 10W (5V, 2A) باستخدام تقنية نقل الطاقة اللاسلكي بالاعتماد على ظاهرة الرنين.

تم تقسيم العمل بالشكل الاتي:

أولاً، تم تصميم نظام لتوضيح ظاهرة تقسيم التردد في نظام WPT بواسطة برنامج ADS حيث تم توضيح تأثير عامل الاقتران على النظام . حيث كلما كانت قيمة التردد أعلى يكون تأثير انقسام التردد عند قيمة أقل من عامل الاقتران للترددات الأقل.

ثانياً، تم تصميم نظام نقل الطاقة اللاسلكي لشحن الهواتف الذكية الحديثة بواسطة برنامج MATLAB حيث تم الأخذ بنظر الاعتبار بعض العوامل التي لها تأثير على كفاءة النظام مثل المسافة وعامل الاقتران وتردد الرنين وإن مدى الترددات التي تم استخدامها هو 50-100 KHz وبعدها تم مناقشة النتائج عند كل تردد والمقارنة بينها من أجل اختيار التردد المناسب. تم الاستنتاج ان دائرة شحن بطارية الهواتف الذكية التي تم تصميمها تكون في أفضل مستويات أدائها عند تردد الرنين 100 KHz حيث كانت كفاءة النظام عندما كانت المسافة بين الجهازين تساوي 30 mm تساوي 76% في حين عند التردد 50 KHz و مسافة 30 mm كانت كفاءة النظام تساوي 71%.

شكر وتقدير

أود ان أقدم جزيل الشكر والامتنان لمشرفي الأستاذ الدكتور أوس زهير
يونس على توجيهاته المفيدة وتشجيعه المستمر لي طوال فترة البحث
له كل الاحترام والتقدير

أتقدم بالشكر لكل أساتذتي في قسم هندسة الالكترونيك على دعمهم
ومساعدتهم المستمرة، فلهم مني كل التقدير.

أود أن أعبر عن خالص تقديري وحبّي لأبي وأمي وزوجي على دعمهم
وتشجيعهم لي طوال فترة دراستي العليا

أخيراً، أقدم شكري لكل من كان له الفضل علي خلال مرحلة البحث ولو
بمساعدة أونصيحة او دعاء

اليهم جميعاً أعبر عن خالص تقديري واحترامي

إقرار المشرف

نشهد بأن هذه الرسالة الموسومة (تقنية نقل الطاقة لاسلكيا للأجهزة المحمولة) تم اعدادها من قبل الطالبة (ريم عماد نافع) تحت اشرافنا في قسم هندسة الالكترونيك / كلية هندسة الالكترونيات / جامعة نينوى، وهي جزء من متطلبات نيل شهادة الماجستير/علوم في اختصاص هندسة الالكترونيك.

التوقيع:

الاسم: أ.م.د. أوس زهير يونس

التاريخ:

إقرار المقوم اللغوي

اشهد بأنه قد تمت مراجعة هذه الرسالة من الناحية اللغوية وتصحيح ما ورد فيها من أخطاء لغوية وتعبيرية وبذلك أصبحت الرسالة مؤهلة للمناقشة بقدر تعلق الأمر بسلامة الأسلوب أو صحة التعبير.

التوقيع:

الاسم: د. محفوظ خلف محمود

التاريخ:

إقرار رئيس لجنة الدراسات العليا

بناءً على التوصيات المقدمة من قبل المشرف والمقوم اللغوي أرشح هذه الرسالة للمناقشة.

التوقيع:

الاسم: أ.د. قيس ذنون نجم

التاريخ:

إقرار رئيس القسم

بناءً على التوصيات المقدمة من قبل المشرف والمقوم اللغوي ورئيس لجنة الدراسات العليا أرشح هذه الرسالة للمناقشة.

التوقيع:

الاسم: أ.د. قيس ذنون نجم

التاريخ:

إقرار لجنة المناقشة

نشهد بأننا أعضاء لجنة التقويم والمناقشة قد اطلعنا على هذه الرسالة الموسومة (تقنية نقل الطاقة لاسلكيا للأجهزة المحمولة) وناقشنا الطالبة (ريم عماد نافع) في محتوياتها وفيما له علاقة بها بتاريخ وقد وجدناها جديرة بنيل شهادة الماجستير/علوم في اختصاص هندسة الالكترونيك.

التوقيع: رئيس اللجنة: أ.م.د. أحمد ذنون يونس
التوقيع: التوقيع: عضو اللجنة: أ.م.د. احمد محمد سلامة
التاريخ: التاريخ:

التوقيع: التوقيع: عضو اللجنة (المشرف): أ.م.د أوس زهير
التوقيع: التوقيع: عضو اللجنة: م.د. محمد ناطق عبد القادر
التاريخ: التاريخ: يونس
التاريخ: التاريخ:

التوقيع: التوقيع: عضو اللجنة (المشرف): أ.م.د أوس زهير يونس
التاريخ: التاريخ:

اقرار مجلس الكلية

اجتمع مجلس كلية هندسة الالكترونيات بجلسته المنعقدة بتاريخ:
وقرر المجلس منح الطالبة شهادة الماجستير علوم في اختصاص هندسة الالكترونيك

مقرر المجلس: أ.م.د. ضياء محمد علي
رئيس مجلس الكلية: أ.د. خالد خليل محمد
التاريخ: التاريخ:



وزارة التعليم العالي والبحث العلمي

جامعة نينوى

كلية هندسة الالكترونيات

قسم هندسة الاكترونيك

تقنية نقل الطاقة لاسلكيا للأجهزة المحمولة

رسالة تقدمت بها

ريم عماد نافع قريشات

الى

مجلس كلية هندسة الالكترونيات

جامعة نينوى

كجزء من متطلبات نيل شهادة الماجستير

في

هندسة الألكترونيك

بإشراف

أ.م.د. أوس زهير يونس الاشقر



وزارة التعليم العالي والبحث العلمي

جامعة نينوى

كلية هندسة الالكترونيات

قسم هندسة الاكترونيك

تقنية نقل الطاقة لاسلكيا للأجهزة المحمولة

ريم عماد نافع قريشات

رسالة ماجستير

في

هندسة الألكترونيك

بإشراف

أ.م.د. أوس زهير يونس الاشقر